Biochimica et Biophysica Acta, 977 (1989) 99–122
Elsevier

BBABIO 43073

Review

Spectroscopy and electron transfer dynamics of the bacterial photosynthetic reaction center

Richard A. Friesner and Youngdo Won

Department of Chemistry University of Texas at Austin, Austin, TX (U.S.A.)

(Received 7 April 1989)

Key words: Electron transfer dynamics; Photosynthesis; Reaction center; Charge separation (Bacterium)

Contents

Abbreviations: RC, reaction center; ET, electron transfer; BChl, bacteriochlorophyll; BPh, bacteriopheophytin; SP, special pair; *Rps., Rhodopseudomonas; Rb., Rhodobacter*; CD, circular dichroism; PVA, polyvinyl alcohol; CT, charge transfer; HS, Hayes and Small; PW, Parson and Warshel; WF, Won and Friesner; ZPL, zero phonon line; ST, singlet-triplet.

Correspondence: R.A. Friesner, Department of Chemistry, University of Texas at Austin, Austin, TX 78712, U.S.A.

Introduction

The elucidation of the structure of two bacterial reaction centers via X-ray crystallography [1–8] has initiated has initiated a profound transformation in research on the primary charge separation steps of photosynthesis. A great deal of the work done prior to these events was concerned with the determination of the identities and location of various components of the reaction center (RC). While some of the results along those lines proved to be quite accurate, the X-ray studies have resolved many of the remaining structural uncertainties definitively. Thus, efforts have shifted to the deduction of function from structure, i.e., a detailed, molecular level specification of the mechanism of light-induced charge separation.

That this task has not proven to be any easy one should not be surprising, any more than, for example, that a microscopic description of source of hemoglobin cooperativity did not immediately arise from the crystal structure of that protein. The remarkable features of the primary electron transfer (ET) event (extreme rapidity down to 4 K, near-unit quantum efficiency) have been quite difficult to reproduce simultaneously in synthetic model compounds [9] (although some progress along these lines has been made), which in any case are not embedded in a protein environment. Thus, the most relevant experimental and theoretical studies have had to deal directly with the complexity of the in vivo system, where a variety of competing possible explanations exist for almost every phenomenon that has been observed. Ultimately, chemical modification [10] and site-directed mutagenesis [11–14] of the RC protein may lead to experiments which are able to select the correct alternative unambiguously. At present, however, the level of control over the structure is not sufficient for this, and many fundamental questions remain to be answered.

In this article, we examine the important issues concerning the RC from a theoretical perspective. Experimental results will in general by briefly described; several reviews covering experimental work in greater detail have appeared recently [15,16,129]. Emphasis will be placed on the interaction of theory and experiment, particularly in the interpretation of spectroscopic experiments of various types.

Section II reviews the RC structure, describing both the photophysical properties of the individual bacteriochlorophyll (BChl) and bacteriopheophytin (BPh) chromophores and the spatial organization of the RC as revealed by crystallographic analysis. Section III discusses the construction of theoretical models (at various levels of sophistication) that are relevant to the spectroscopic and ET properties of the RC. The performance of various models in explicating experimental data is examined in sections IV (time-independent spectroscopy) and V (ET dynamics). The last section provides a brief conclusion.

II. Basic features of the reaction center

II-A. Reaction center structure and the fundamentals of charge separation

The bacterial RC is a globular, multiple subunit protein which is embedded in a photosynthetic membrane. Light is typically first absorbed in the native organism by an antenna protein, which contains Chl-type chromophores but lacks the machinery to separate charge. The excitation then migrates very rapidly via energy transfer to the RC, where it is trapped by a low-lying excited state of a pair of BChl molecules, designated the special pair (SP).

Highly refined crystal structures of the RC currently exist for two photosynthetic bacteria, *Rps. viridis* [1–3] and *Rb. sphaeroides* [4–8,129]. While there are some differences in both the amino-acid sequence and the porphyrin chromophores which carry out the charge separation, the three-dimensional crystal structures, optical spectra, and electron transfer dynamics are in most ways quite analogous. A third strain of bacteria, *Rb. capsulatus*, is also of importance because it is the first system in which site-directed mutagenesis experiments have been carried out [11–14] (genetic work on other organisms is currently in progress in various laboratories). The amino-acid sequence and photophysical properties of this organism are very similar to the first two [130], leading to the assumption (made by most workers) that the structure is also homologous.

Fig. 1 displays the arrangement of the six porphyrin chromophores in the X-ray structure of *Rps. viridis* RC. The subscripts L and M (following Deisenhofer and co-workers) refer to the corresponding protein subunits. The chromophores themselves display an approximate C_2 symmetry with regard to the M and L subunits, with three almost identically positioned chromophores forming a 'branch' along which charge separation might occur. Remarkably, only one of these branches (the L branch) appears to be active in charge separation in naturally operating reaction centers. Determination of the cause of this asymmetry is one of the major unsolved tasks in unraveling the workings of the RC. To answer this and other analogous questions in a truly satisfactory fashion, one must obviously consider the details of the protein structure and the effect of this structure upon the chromophores. As most suggestions along these lines are at present speculative, the topic will not be discussed at length in this review.

As described above, any absorbed light quantum ultimately moves (via rapid energy transfer) to the lowest excited state of the special pair, the two constituent BChl molecules of which are designated P_L and

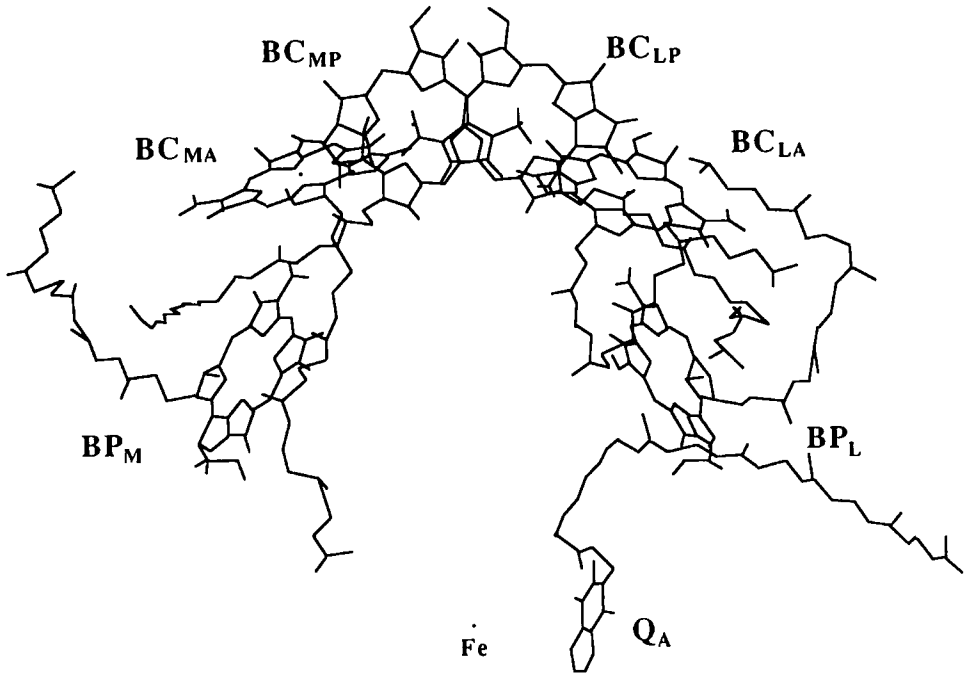

Fig. 1. The chromophore structure of the *Rps. viridis* RC after Ref. 1. The four bacteriochlorophyll *b* and the two bacteriopheophytin *b* molecules are arranged in two branches, L and M. The pseudo-C_2 rotation symmetry axis is aligned vertically in the plane of the paper, running through the special pair to non-heme iron atom. The periplasmic side of the membrane is near the top and cytoplasmic side is near the bottom of the structure.

P_M. These molecules are strongly coupled electronically as evidenced by, for example, their circular dichroism spectrum [17,18], and will be the focus of much of the forthcoming discussion. In roughly 3 ps (the precise time constant depends weakly on temperature and on the species [19,20]), an electron is transferred to the BPh on the L branch of the protein (labelled H_L in Fig. 1); the free energy gap between the donor and acceptor states is known to be approx. 0.17 eV from delayed fluorescence measurements [21] (measurements based on decay of the triplet state in high magnetic fields yield the somewhat larger value of 0.26 eV [131]; the source of this discrepancy remains to be understood). The role of the 'accessory' (or 'intermediate') BChl molecule B_L is presently unknown and a subject of great controversy. The center-to-center and edge-to-edge distances of the six pigments are given in Table I; these numbers immediately reveal why one would expect B_L to mediate electron transfer between the SP and H_L. The failure to observe bleaching of B_L in femtosecond experiments has been one of the great surprises of the past few years [22–24,119–121], and has made construction of a suitable ET mechanism a severe challenge.

In the remainder of this review, we will principally be concerned with the active (L) branch. Therefore, the subscript L on the symbols B and H will be suppressed; any reference to these molecules should be assumed to refer to the L branch unless an M subscript is appended. The symbol P is conventionally used to designate the special pair complex, e.g., P* refers to the lowest excited state of the SP (located at 960 nm at room temperature in *Rps. viridis*). Consequently, P_L and P_M will be used to designated the individual L or M constituents of P, and lack of a subscript will indicate the dimer.

At room temperature, an electron is transferred in about 200 ps from H^- to Q_A (the first quinone acceptor) [16,25], whereupon a series of considerably slower steps complete the processing of the light-induced redox potential into chemical energy. The state $P^+Q_A^-$ is extremely stable against charge recombination, so that this electron transfer can in practice be considered irreversible (one can observe this recombination, on the millisecond timescale, if electron transfer to the sec-

TABLE I

Parameters relating neighboring chromophores of RC from Rps. viridis

Data obtained from the X-ray coordinates of Deisenhofer and coworkers. The atom pair that gives the closest distance is denoted in the parentheses.

Chromophores	Distance between ring centers (Å)	Edge-to-edge distance (Å)	closest contact (Å)
P_L–P_M	7.0	2.5 (CHC–CHC)	2.2 (Mg–OBB)
P_L–B_L	10.4	5.0 (CAD–C3C)	2.6 (CP4–CHC)
P_M–B_M	10.8	6.0 (C3C–CAD)	3.8 (OBD–CBC)
B_L–H_L	10.2	4.8 (C1B–C2B)	3.3 (O2A–OBB)
B_M–H_M	11.0	5.7 (C2B–C2B)	3.2 (CP9–CMA)
P_L–H_L	16.5	9.5 (C2A–C2C)	3.0 (CP3–CBB)
P_M–H_M	17.0	9.8 (C2C–C2A)	2.4 (O2A–CP14)

ondary quinone Q_B is blocked). While the subsequent reactions are of considerable interest, they are not really relevant to charge *separation*, and hence will be deemed to lie outside the scope of this review.

A completely satisfactory theoretical description of the RC would involve the ability to carry out accurate first principles calculations of the ET rate constants and spectroscopic observables from the RC structure with no adjustable parameters. This is at present a formidable task because of (a) the size and complexity of the the RC; (b) the wide range of timescales present in the dynamics (c) the highly quantum mechanical (possibly coherent) nature of many of the relevant processes (d) uncertainties in the structure, particularly with regard to the chromophores, due to limitations of the X-ray refinement procedures. The impossibility of a brute force approach implies that knowledge of the structure is in this case not sufficient to immediately specify function, and that approximate models have to be constructed and evaluated. The difficulty of the latter task will be apparent in the sections that follow.

II-B. Photophysical properties of the porphyrin chromophores

The photophysics of porphyrins and related molecules have been studied by physical chemists for many years, most notably by Gouterman and co-workers [26]. We briefly review here some of the relevant facts concerning the low-lying excited states; the reader is referred to Ref. 26 for more detailed information. While a great deal is now known about this class of molecules, we are far from being able to produce a complete theoretical description, even for isolated chromophores.

Many of the simplest porphyrins possess D_{2h} or D_{4h} symmetry, which is reflected in the excited state manifold. The basic excited configurations involve promotion of an electron in the π system to an unoccupied orbital. There are four important zeroth order excited states, which are grouped into two pairs of degenerate transitions polarized in the macrocycle plane. The two zeroth order states comprising each pair undergo substantial configuration mixing, yielding an (approximately) symmetric state at high energy (B state) and an antisymmetric state at low energy (Q state). The symmetry considerations imply that the B states have a considerably higher oscillator strength than the Q states, as is observed in porphyrins with high symmetry. One-phonon vibronic components of the Q states, which acquire intensity via vibronic borrowing from the B manifold, can also be seen in the absorption spectrum.

The chromophores which make up the active part of the bacterial RC are complicated porphyrins in which the symmetry is broken in several ways. This causes a reorganization of the configuration interaction between the zeroth order states comprising the Q and B manifolds and splits the in-plane degeneracy of each manifold as well. One then emerges with four excited states spanning the visible and near-infrared region: Q_y, Q_x, B_y, and B_x (the subscript refers to the polarization of the transition in the macrocycle). The Q_y state is always lowest in energy (750–1000 nm) for the molecules that we will consider, followed by the Q_x state (500–600 nm); both of these states still have an oscillator strength less than that for the B, or Soret bands (approx. 400 nm), although the Q_y has substantially increased amplitude as compared to highly symmetric porphyrins. Our attention will primarily be focused on the Q_y states of the various chromophores, as it is these levels that are believed to be most intimately involved in charge separation.

In the RC, the optical and redox properties of the pigments are considerably modified by the protein environment and by interchromophore coupling. The most striking effects are large red shifts of the Q_y bands as compared to monomer spectra in solution. The origin of these shifts is still controversial, with both chromophore-protein and chromophore–chromophore interactions proposed as the source [26–29]. It seems likely that both mechanisms make some contribution, but many details remain to be worked out. Similarly, in some cases (e.g., the SP) the redox properties of the chromophores are substantially modified from monomer solution values. As will be seen below, the energies of various possible interchromophore charge transfer states are of critical importance in evaluating models for charge separation.

The properties described above depend exclusively upon the wavefunctions of the various electronic states of the chromophores. In order to properly analyze optical spectra and electron transfer dynamics, we must also understand how these states are coupled to intramolecular and medium nuclear motion. The simplest type of coupling is an alteration of the equilibrium geometry of a molecule upon change of electronic state. This is ordinarily expressed in terms of the Franck-Condon factor for the transition (which is proportional to the magnitude of the displacement of the equilibrium position of the coordinate in question) of each vibrational degree of freedom. Higher order modifications of the potential surfaces (frequency shifts, mode mixing or Duschinsky rotations, anharmonic effects) can also in principle significantly affect observables.

III. Theoretical models of the reaction center

Any theoretical model of the RC must deal with three basic questions: (1) modeling of the chromophores, including chromophore-chromophore interactions; (2) modeling of the protein environment; (3) chromophore-protein coupling. The problem can be di-

vided further into consideration of electronic and vibrational motion.

The optical spectra of the RC chromophores could be obtained from the electronic energy and potential surface of the ground state and each relevant excited state. To lowest order, knowledge of only the equilibrium geometry of the nuclei in each state is required (this allows computation of Franck-Condon factors for optical transitions). Calculation of the electron transfer dynamics necessitates, in addition, knowledge of the exchange coupling matrix elements between the initial donor (in this case, P*) and charge separated configurations, as well as any intermediate virtual configurations which play a role in mediating charge separation.

An accurate evaluation of these quantities is a demanding task even for an isolated porphyrin molecule or synthetic model complex containing a few chromophores. The presence of the protein environment amplifies the difficulties considerably, particularly because it almost certainly plays a crucial role (e.g., in inducing asymmetry in the L and M branches).

III-A. Chromophore electronic structure

III-A.1. Methodology

The most fundamental theoretical approach to the RC electronic structure problem would begin by carrying out ab initio quantum mechanical calculations to determine the wavefunctions and energies of the electronic ground, excited and charge-separated states (and the coupling matrix elements between these states) of the RC complex, holding fixed all of the nuclear coordinate in their equilibrium positions. Accurate results could no doubt be obtained if one included a sufficient number of amino acid residues around the cofactors and utilized a large basis set and a high level of electron correlation. Unfortunately, such a calculation is at present prohibitively expensive (by perhaps 10 orders of magnitude), even with the latest generation of supercomputers. While a few ab initio calculations on a single chlorophyll molecule including limit configuration interaction have been performed recently [30], these results are far from being relevant to the crucial issues involved in charge separation. At a minimum, three to four more orders of magnitude in computational efficiency will be required before relevance is attainable. This may come to pass over the next decade, particularly if significant algorithmic improvements in ab initio computer codes are possible as has been suggested in recent work [31–34].

An alternative to ab initio electronic structure calculations is to employ semiempirical methods. These approaches are able to handle large systems with reasonable efficiency and are capable of yielding useful results if the problem at hand meshes suitably with the parametrization used in the semiempirical method. Unfortunately, this last condition is far from easy to satisfy, particularly for complicated systems like the RC.

A third alternative is to model the chromophore properties from experimental data on in vitro molecules (e.g., BChl in solution or in a hydrocarbon matrix). This type of approach is often employed in conjunction with semiempirical or ab initio methods. Given the capabilities of the latter methods, such corrections are clearly essential if one wishes to attain a degree of accuracy sufficient to address real questions about the RC.

Finally, one can directly construct phenomenological models which adequately reproduce the properties of the RC. The dangers of this approach are obvious; it can easily degenerate into an exercise in parameter adjustment. On the other hand, it should be pointed out that the overwhelming majority of successful theoretical models for complex systems (for example, in theoretical solid state physics) have incorporated a substantial phenomenological component. As an illustration, the BCS model of superconductivity [35] (one of the most striking successes of condensed matter theory over the past forty years) is entirely phenomenological, as are the great majority of models being put forth to explain high-temperature superconductors [36].

Of the methods applied to the RC to date, the semiempirical calculations are the most difficult to assess in terms of intrinsic, a priori reliability (this issue does not arise for phenomenological models, which are by their nature retuned for each experimental system). The crucial question is not the general utility of the methods but rather their suitability for evaluating quantities relevant to charge separation in the RC. While no definitive conclusions along these lines can be drawn at present, it is at least possible to delineate the difficulties faced in this enterprise.

III-A.2. Semiempirical electronic structure calculations

A wide variety of semiempirical calculations have now been carried out for RC chromophores; these have been based on versions of the QCFF-PI [37–39], INDO [29,40–42], PPP [43], and CNDO [44] methods, among others. The results of most of this work have recently been reviewed in some detail [45]. Our objective here is therefore to present a critical overview, rather than repeating the descriptions given in Ref. 45

Calculations relevant to the RC can be divided into three basic types. First, one can study monomeric BChl in the gas phase, with the objective of calibrating the methodology. Second, two or more interacting BChls can be investigated. Finally, the protein environment can be incorporated, either by explicit representation of nearby amino acid residues or via partial charges.

Comparisons with both optical and magnetic resonance experiments can be undertaken. For the former, the energies of low-lying excited states and corresponding dipole strengths are required, while the latter de-

pend upon evaluation of the electron density in various molecular orbitals. To address issues connected to charge separation, one must determine the energies of oxidized and reduced species and the exchange coupling matrix elements between localized states on the different chromophores.

A reasonable level of agreement between theory and experiment has been obtained for electron spin densities, for example by Plato and coworkers [42]. However, these workers developed a version of INDO that is specially parametrized to yield good agreement for spin densities of porphyrins. As the accuracy of semiempirical methods is highly dependent upon the method of parameterization, there is no guarantee that is similarly good results are available for other properties from the same computational approach.

Prediction of optical properties, even for isolated monomers, is much less satisfactory. Errors of 0.5 eV in excitation energies and factors of 2 in dipole strengths are not atypical. Such errors are often corrected by empirical scaling formulas. Again, however, there is no guarantee that the scaling used for a particular set of energy levels will apply in other, more complex situations. For example, in predicting energy shifts upon alterations of the molecule in some fashion (so that the absolute energies are not required), large disagreements between different methodologies are obtained, e.g., in Ref. 29 a 350 cm^{-1} blue-shift, and in Ref. 38 a 1400 cm^{-1} red-shift, is obtained for the energy shift of the Q_y state of BChl due to the rotation of an acetyl group of the molecule.

The most important quantities from the standpoint of charge separation are the exchange coupling matrix elements and the energies of the various possible charge transfer configurations. As these parameters are in general not directly accessible experimentally, is is essential to assess the validity of the semiempirical electronic structure methods as a priori predictive approaches. Unfortunately, the heuristic uncontrolled nature of the approximations makes it impossible to do this in a systematic fashion. What can be observed is that the values obtained by different approaches differ widely, e.g. exchange coupling matrix elements in Refs. 39 and 43 disagree by as much as a factor of 10. Given the performance in computing optical spectra, and the fact that there have not been demonstrations that the methods can accurately obtain these sorts of quantities when applied to simpler, less demanding systems, a degree of skepticism would appear to be warranted in current applications to the RC. The additional question of whether the protein environment has been incorporated in adequate fashion (there is no independent evidence to indicate that it has been) is a further cautionary note.

A final (but quite significant) difficulty is caused by the uncertainty in the atomic positions of the chromophore atoms due to lack of resolution in the x-ray structure. Even if we were to assume that existing semiempirical methods are capable of accurately computing energetic parameters at a given nuclear configuration, there is a high sensitivity of the results to the details of the chromophore geometry (e.g., see Ref. 41). One can imagine refining the geometries by minimizing the semiempirical energy or by using molecular mechanics force fields. The former procedure clearly takes one outside of the domain of parametrization of methods like INDO; the latter would require accurate force fields for excited or ionic states of the porphyrin macrocycles, which presently do not exist. A solution of this problem necessitates developments beyond improvement in electronic structure methodology, and is likely to remain a barrier to accurate modeling of electronic matrix elements for some time to come.

The above discussion should not be taken to imply that existing semiempirical electronic structure calculations on the RC are useless or hopelessly wrong. Indeed, many interesting hypotheses have been developed as a consequence of these calculations, and some agreement with experiments on the RC have been obtained. A good example of the latter is the evaluation of the electrochromic shift of B upon charge separation by Eccles et al. [44] and Hansen et al. [40]. Some of the more speculative modeling – e.g., determination of the ratio of exchange couplings on the L and M branches in Ref. 46, demonstration of the sensitivity of the red shift of P* to the conformation of the SP molecules by Barkegia et al. [41], and the study of the interaction of CT configurations with the P* band by Parson and Warshel [37,38] – may also prove to be correct

Rather, the main point of this section is that these approaches do not have, in the opinion of the authors, a privileged position with regard to constructing models of the electronic coupling in the RC. The only plausible way to validate any such models at present is comparison with experiment, in particular simultaneous explanation of a number of phenomena with the same model. The evaluation of the success of a model in this light should proceed independently of how it is constructed.

III-B. Protein environment

As in the case of chromophore electronic structure, one is essentially faced with the choice of developing a phenomenological representation of the protein environment or of attempting to construct a detailed atomic level model. The former approach corresponds to the usual treatment employed by condensed phase spectroscopists, and entails a description in terms of damping constants, relaxation parameters, frequency shifts, etc. The latter involves the utilization of molecular mechanics models of proteins, which have undergone rapid development over the past ten years. We

defer discussion of phenomenological models to a later section, and focus on prospects of extracting useful information from molecular models of the reaction center.

III-B.1. Detailed atomic level models

During the pas decade, there has been an explosive growth in the application of molecular modeling techniques to biological systems. Beginning with the work of Lifson and coworkers [48–50] and Karplus and coworkers [51], detailed atomic level models of protein structure and dynamics have been produced and utilized to simulate a wide variety of experiments, e.g., the thermodynamics of drug binding [52], X-ray temperature factors [53], NMR linewidths due to the hindered rotation of methyl groups [54], and electrostatic free energies of ionizable groups in proteins [126–128].

It is very difficult at this point in time to objectively assess the performance of these models. There is no question that one can now qualitatively visualize interactions and dynamics in proteins, particularly with the rapid improvement of graphics software and hardware. On the other hand, the quantitative predictive power of protein simulations – which must critically depend upon the reliability of the potential energy functions – is far from being rigorously demonstrated. This is particularly true when considering the effects of prosthetic groups (for which the parametrization of the relevant energy surfaces is not routine) and for systems where quantum mechanical coupling of several potential surfaces must be taken into account. As these features dominate the problem of charge separation in the RC, the ability of such simulations to resolve the important questions presently at issue is unclear.

Several groups have now carried out molecular dynamics simulations of the RC [39,47,55–57]. In order to assess the reliability and value of these calculations with regard to primary ET dynamics, it is useful to consider the questions that one would like a detailed, atomic level model to answer, and the possible sources of error in the simulations which might render such answers inaccurate. Some important questions are:

(1) What are the energies of the chromophore electronic configurations (including excited states and charge transfer states) in the protein environment?
(2) How does the environment affect the electronic coupling matrix elements between chromophores?
(3) How does the protein reorganize upon charge separation? In the language of Marcus theory, this is quantitatively expressed via a single number, the reorganization energy. In the context of understanding charge separation in the RC, one would like a more detailed picture of the adjustments made by the protein and chromophores in the course of the primary process.
(4) What is the overall ET rate constant as a function of temperature?
(5) How does the calculated rate depend on various model assumptions concerning the crucial parameters (e.g., off-diagonal electronic matrix elements)?

Clearly, one must get the first three of these right before the answer to the fourth is meaningful.

Some issues which might make realization of the above objectives difficult are:

(A) Can one accurately parametrize (a) the chromophore force fields and partial charges (b) chromophore-protein interactions (both electrostatic and nonbonded van der Waals)? The question is phrased in this manner because there do not presently exist 'standard' force fields for chlorophylls. Note that the parameterization in principle must be accomplished for the excited and charge separated states of each chromophore as well as for the ground state, and that, as discussed in subsection III-A, electronic structure calculations on these molecules (which might assist in the parameterization) are not highly accurate. There are also questions concerning the accuracy of existing force fields and partial charges for the protein itself.
(B) Does one have enough computational power to obtain converged results for free energies and other equilibrium quantities, even at the classical level? The system is quite large, making simulations rather expensive.
(C) What is the quality of the quantum mechanical couplings between potential surfaces inserted into the model? These numbers must come from electronic structure calculations which, we have argued, are not capable of producing them reliably. Note that this difficulty probably precludes obtaining an unambiguous answer to question (4) but does not prevent the achievement of more modest goals, e.g. those in (3) or (5).
(D) Can one carry out mixed quantum-classical simulations accurately when the classical subsystem is so large and complicated? This is a very difficult theoretical problem, which has not been solved definitely even for small, few atom systems.

We now describe the two simulations that have been carried out to date in the context of the above questions. Here, we are concerned principally with issues of methodology, i.e., how much can one learn about charge separation from a detailed atomic level model of the RC, given the limitations of present simulation technology; a further discussion of some of the results of these simulations will appear in Section V.

Treutlein et al. [56,57] have carried out molecular dynamics and electrostatic free energy calculations using the *Rps. viridis* coordinates. They parametrized chromophore partial charges via MNDO semiempirical electronic structure calculations for the ground and charge

separated states; it is not obvious from their paper how the covalent part of the chromophore force field was modeled. Two simulations were then run; one with the RC in the ground state and one in the charge separated (P^+H^-) state. The average structures of the protein before and after electron transfer were investigated. In another calculation, the authors monitored the energy gap between the electronic configurations P* and P^+H^- during simulations in each state. In the context of conventional (Marcus) electron transfer theory, a crossing of the energy levels signals the possibility of electron transfer. Such crossings were in fact observed, thus indicating that protein fluctuations in the model were capable of producing the appropriate near degeneracies of the donor and acceptor states.

The objectives of these calculations were primarily qualitative, e.g., actual calculation of the ET rate was not attempted, and high accuracy was not claimed for the diagonal energies of the participant electronic states, due to uncertainties in the relevant chromophore properties. The principal results were the observation of level crossings due to protein fluctuations (described above) and a physical picture of how the protein alters its conformation upon charge transfer.

Another molecular dynamics simulation of RC dynamics has been carried out by Parson, Warshel, and coworkers using the X-ray coordinates for the *Rb. sphaeroides* RC obtained by the Argonne group [39,47,55]. The model developed by these investigators is considerably more elaborate than that of Treutlein et al., with regard to the diagonal electronic energies, off diagonal couplings, and chromophore force field. The first of these was parametrized by using solution electrochemical measurements as a starting point followed by free energy perturbation theory to incorporate the effects of the protein environment, while the last two were obtained from QCFF-PI semiempirical calculations. A semiclassical molecular dynamics method based on a Fourier transform of the time-dependent energy gap [109] was then used to evaluate the ET rate of primary electron transfer. The reorganization energy of the protein upon charge separation was also calculated.

Both calculations produced interesting (although rather different!) observations concerning protein reorganization upon charge separation (a more explicit comparison of these results is not possible at present, due to the absence of quantitative details, particularly in Refs. 56 and 57). This is an issue for which one would expect simulations to be capable of yielding reasonable results, as the dependence upon parameterization should not be overly sensitive. Similarly, evaluation of the electrostatic contributions to the energies of the electronic states is plausible, although the accuracy obtainable for the gas phase reference energies (estimated crudely in Ref. 56, claimed to be determined rather precisely in Ref. 55) is difficult to assess. The convergence of the simulations appears not to be a limiting factor, although this was not demonstrated unambiguously by either group.

On the other hand, the off-diagonal coupling matrix elements and description of the electronic states of the SP are subject to the same uncertainty as in phenomenological models. In Refs. 39 and 55, the protein environment was not used in obtaining these quantities, and the quantum chemical calculations themselves were done at an unreliable level of theory. As these factors are crucial in determining the efficiency of charge separation, it is certainly not possible to definitively resolve controversies concerning the ET mechanism by appeal to the simulation results. From this point of view, we can regard these results as numerical experiments with a complicated model which can hopefully provide insight into the factors which control the ET dynamics.

III.B.2. Phenomenological models

In a general sense, all existing theoretical models of the RC are phenomenological, in that they are not derived by solving the Schrödinger equation for the entire protein from first principles. However, we shall use this term in a more restricted way, to refer to relatively simple approximate models constructed primarily by fitting assumed functional forms to experimental data. Such a model is most useful either if it is obviously correct (in which case the extracted parameters can immediately be assigned a physical interpretation) or if a sufficient set of experimental data can be subsumed by the same model, thus providing cross checks on the model assumptions. Otherwise, an adequate fit only demonstrates the model's consistency; if there is enough flexibility in the functional form as compared to the set of experimental data, almost any hypothesis can be made consistent. A typical prevailing situation for complex problems in chemical physics is that several competing models exist, which their adherents suitably modify as new experimental results are reported. One purpose of the present review is to critically present the various competing pictures and to assess the prospects of distinguishing them in the future.

The simplest type of phenomenological model for the RC consists of electronic parameters describing the energies, dipole strengths, and electronic couplings of the relevant chromophore states. Such models yield delta-function lines for optical spectra unless parametrized lineshape functions are also constructed. To obtain electron transfer rate constants, one must in addition assume either a reorganization energy (in Marcus theory), or, additionally, specific couplings to molecular or medium vibrational modes.

Fischer and co-workers have extensively employed such an approach to model a variety of optical spectra from the RC, fitting experimental profiles by empirically adjusting the electronic state energies, dipole

strengths, SP interactions, and individual lineshapes of each transition [28,58,59]. Their calculations demonstrate that a simple exciton picture, utilizing the dipole directions obtained from the RC crystal structure, can provide intensity distributions that are roughly consistent with the experimental measurements.

Many groups have used a simple phenomenological framework to explore proposals for electron transfer dynamics; among these are Marcus [60–63], Michel-Beyerle and co-workers [64–66], and Won and Friesner [67]. Additionally, this approach has been adopted in most experimental papers on the subject. A further discussion of this will be presented in subsection V-B.

A more complex phenomenological model is one which explicity incorporates vibrational as well as electronic degrees of freedom. In this approach, one typically specifies a set of strongly coupled modes which are to be treated explicity; the modes are characterized by a frequency and an equilibrium geometry shift in the excited or ionic states of a chromophore; frequency shifts or anharmonic couplings in the excited state are usually neglected or treated phenomenologically. Won and Friesner have developed such a model and used it to study optical spectra and photochemical holeburning [68–71]. Fischer and co-workers have proposed an explanation of the temperature dependence of the P* band via a vibronic model [72], while Hayes and Small have constructed displaced harmonic oscillator models to explain photochemical holeburning results [73,74]. We briefly describe the Won and Friesner model here, as results from it will be discussed below in some detail.

Each porphyrin chromophore is assigned a set of intramolecular vibrational modes. The Franck-Condon factor (equilibrium displacements) for each mode in the Q_y state are estimated from supersonic jet experiments on free base porphin [75] and from site selection experiments on Chl *a* embedded in a hydrocarbon matrix [76]; those for charge transfer states are obtained from electronic structure calculations of Warshel [77]. Each vibronic line is given the same phenomenological width, arising from inhomogeneous broadening, acoustic phonons, anharmonicity, etc.

As described above, this model is not capable of reproducing the anomalous width of the P* band, or its temperature dependence. Consequently, Won and Friesner include a single intermolecular mode of the SP (which is likely to be relative motion of the two macrocycles) which is assigned a relatively large Franck-Condon factor, i.e., the equilibrium intermolecular separation of the SP is postulated to change significantly upon excitation, a particularly likely state of affairs if there is internal separation of charge in the P* state, as is argued below. The parameters of this mode are taken to be temperature dependent. The magnitude of the vibronic coupling parameter is adjusted to reproduce the homogeneous linewidth obtained from holeburning experiments. Further discussions of the validity of the various approximations involved in the model and its performance as compared to experiment can be found in Refs. 68–71 and, in abbreviated form, below.

IV. Optical spectroscopy of the reaction center

A wide variety of spectroscopic experiments have been carried out on the reaction center. We will divide these into three classes. The simplest class of experiments are those involving 'conventional' types of absorption measurement, including absorption, polarized absorption, linear dichroism, circular dichroism and resonance Raman. The second class consists of 'unconventional' but still time-independent techniques; at present, this includes Stark effect studies, holeburning measurements, and electric field effects on oriented monolayers of RCs. Finally, numerous time-resolved transient absorption measurements have been made under a variety of conditions. We will also place fluorescence quantum yield studies in this last class, as these bear primarily on ET dynamics.

In this section, we discuss modeling and interpretation of the data set obtained from time independent experiments; time-resolved experiments will be considered in subsection V-A. In some cases, the information obtained is only indirectly related to charge separation, while in other cases one must assume a primary ET mechanism to compute the desired observable. A global assessment of the performance of proposed charge separation mechanisms will be deferred to the next section; when this issue arises here, we will in general briefly mention the potential problems faced by each type of mechanism.

An additional set of experiments which are relevant to the ET dynamics are those involving magnetic field effects [79–82]. Because of a lack of space, these will receive a less detailed treatment in this review; the most important of them from the standpoint of understanding the ET dynamics will be introduced.

We restrict the bulk of our discussion of optical spectra to the Q_y region of the RC spectrum, as it is this region which is of the most direct relevance to charge separation. Thus, techniques which have primarily been applied to the Soret region (e.g., resonance Raman) will not be examined in detail.

IV-A. Absorption, polarized absorption and circular dichroism

The experimental absorption spectrum of the RC of *Rps. viridis* at 4.2 K [83] in the 700–1050 nm spectral region is displayed in Fig. 2, along with the theoretical fit obtained by Won and Friesner [68,71] using the vibronic model described in subsection III-B.2. The assignment of all of the peaks in the spectrum has now

TABLE II

Rps. viridis low temperature absorption band assignments

788 nm	Bph_M Q_y transition
810 nm	Bph_L Q_y transition
833 nm	two accessory BChl-*a* Q_y transition
850 nm	upper excitonic component of the special pair
996 nm	lower excitonic component of the special pair

beeen accomplished, principally by utilizing linear and circular dichroism data as well as absorption measurements. Table II lists the wavelength maximum and assignments for each identifiable band. These assignments are generally agreed upon by all investigators at this point in time, with the possible exception of the shoulder at 850 nm, as discussed below.

A number of unusual features (as compared to, e.g., spectra of BChl and BPh in solution) are immediately apparent. The most strongly altered bands are those of the special pair. A strong exciton splitting of about 850 cm^{-1} separates the (+) and (−) exciton components of the dimer. The identification of the shoulder at 850 nm as the (+) exciton components of the SP has been controversial, but has now been accepted by most workers in the field. Experimental evidence comes from linear dichroism measurements [84–86], Stark effect measurements [87,88], and from kinetics measurements which show that excitation into the 990 nm band produces an instantaneous bleaching of the shoulder (but nowhere else in the absorption band) [19]. From a theoretical viewpoint, Eccles et al. [44] have made this assignment based on semiempirical electronic structure calculations, while Won and Friesner [68–71] have deduced it from simultaneous phenomenological simulations of several optical properties.

In addition to the splitting, the center of gravity of the SP absorption is shifted about 125 nm to the red of BChl absorption in solution [89]. Note that the monomer BChl absorption is also substantially shifted (to about 833 nm), although not as far as is the dimer. A final anomalous feature is the width of the P* band, which is roughly twice that of the BChl monomer band.

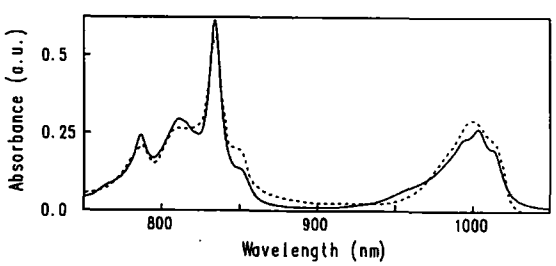

Fig. 2. Comparison of the 4.2 K *Rps. viridis* RC absorption spectrum calculated from WF vibronic coupling Hamiltonian (solid line) with the experimental result of Vermeglio et al. [83] (dotted line).

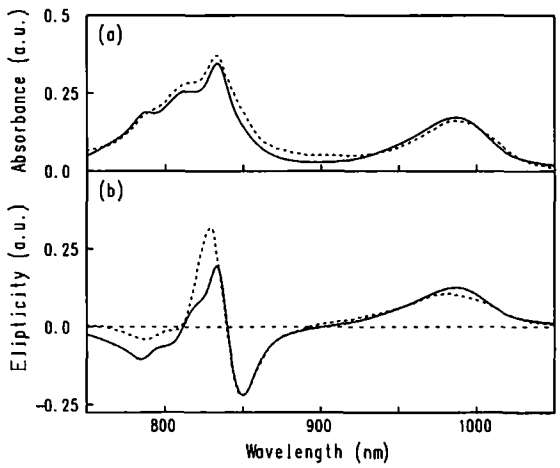

Fig. 3. Comparison of the 100 K *Rps. viridis* RC (a) absorption and (b) CD spectra calculated from WF vibronic coupling model (solid line) with the experimental result of Shuvalov and Asadov [17] (dotted line).

The vibronic coupling theory used to generate Fig. 2 employs adjustable peak positions and dipole strengths [68], so not much importance should be attached to the agreement along these lines in Fig. 2. However, only one phenomenological line broadening parameters was used for the entire spectrum; all Franck-Condon factors were obtained from independent simulations of monomer vibronic intensities, while the intermolecular coupling for the SP was determined from holeburning simulations, as described below [71]. Note that this procedure yields a good reproduction of the asymmetry of the P* band and of the profile of the upper dimer component at 850 nm; this indicates that the vibronic parameter set is a reasonable one.

Figs. 3 and 4 displays fits to the experimental polarized absorption and circular dichroism spectra of

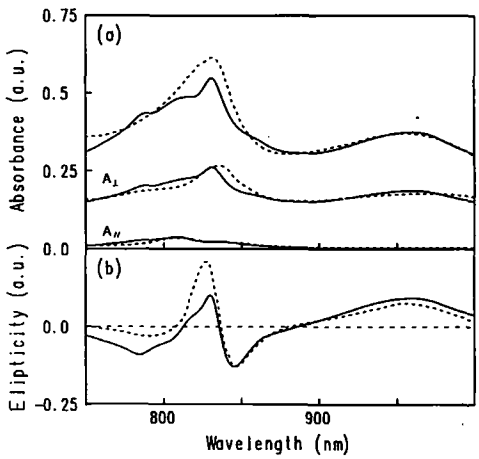

Fig. 4. (a) The room temperature theoretical *Rps. viridis* RC absorption spectrum compared to the experimental result of Phillipson and Sauer [18] (dotted line), and polarized light absorption spectra compared to experimental results of Zinth and co-workers [90] (dotted lines). (b) Comparison of the calculated 297 K CD spectrum with the experimental result of Phillipson and Sauer [18] (dotted line).

the RC using a vibronic coupling model identical to the one employed for absorption at the corresponding temperature (see below); these results provide some cross checks on the validity of the model. In particular, input of the experimental aggregate geometry leads reasonable agreement for polarized spectra, while the line profiles continue to be consistent with the vibronic coupling model.

The phenomenological exciton calculations of Fischer and co-workers also display similar agreement for a variety of experiments; this provides some confirmation of the validity of that approach as well. In fact, there is no conflict between the exciton and vibronic results at this level; the latter simply provides a microscopic interpretation of the numerous adjustable linewidth parameters used in the former. The number of such parameters that are explicity varied is actually considerably smaller in the vibronic theory, because the great majority of parameters are obtained from an independent analysis of monomeric spectra.

A final question concerns the temperature dependence of the 990 nm band. An extraordinarily large blue shift and broadening of this peak are observed as the temperature increases from 4 K to 300 K. This phenomenon has been quantitatively documented by Kirmaier and Holten [91], who employed a single type of sample preparation (PVA films) for all measurements. The last condition is important because the P* band also exhibits a remarkable sensitivity to external features like solvent and rate of cooling; for example, the position of the absorption maximum and various magnetic properties depend upon these factors [92].

The magnitude of the spectral changes cannot be reproduce if one assumes a simple Franck-Condon (linear coupling) displament of the excited state potential surface. The inclusion of quadratic coupling (frequency shifts) in the excited state can produce some additional effects, but still leads to difficulty in explaining the shift in peak position [72].

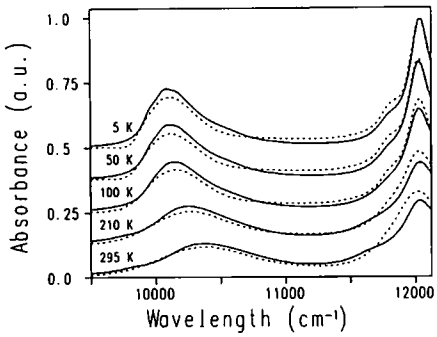

Fig. 5. Comparison of the *Rps. viridis* RC absorption spectra calculated from Green's function of the WF thermal expansion model Hamiltonian (solid lines) with the experimental results of HK (Ref. 91 and personal communication) (dotted lines) at various temperatures. See Table III for the listing of parameters as a function of temperature.

An alternative picture involves an alteration in the excited state equilibrium geometry of the special pair as a function of temperature [93]. The previously described heterogeneous behavior of the P* bands suggests that the potential surface of the dimer is floppy and anharmonic. At low temperatures, the SP molecules can be trapped (depending on cooling rate) in a single potential well in which they are in their closest proximity. At higher temperatures, the average distance between the chromophores in the excited state is postulated to increase (the ground state equilibrium geometry probably alters as well; in this simple picture, we assume that this alteration is less important that that for the excited state). This leads to the prediction that the exchange energy and red shift of the center of the dimer band (due to diagonal exciton interactions) should both decrease, and that the vibronic coupling constant of the SP intermolecular mode should increase (due to the presumed increase in the difference between the ground and excited state geometry).

Fig. 5 displays simulations in which the above three parameters are allowed to vary with temperature so as

TABLE III

Rps. viridis absorption spectra simulation result as a function of temperature

Temp. (K)	Peak position		FWHM		E_p (cm^{-1})	J^* (cm^{-1})	g_p (cm^{-1})	γ (cm^{-1})
	Exp.	Theo	Exp.	Theo.				
5	10107.5	10075.0	467.0	467.6	11083.0	837.0	115.0	75.0
20	10097.5	10075.0	487.0	479.4	11084.0	835.0	115.0	80.0
35	10115.0	10100.0	496.0	496.1	11086.0	832.0	117.5	83.5
50	10112.5	10100.0	499.0	500.1	11088.0	830.0	117.5	85.0
76	10137.5	10125.0	523.0	523.8	11092.0	825.0	120.0	90.0
100	10157.5	10150.0	556.0	550.5	11098.0	818.0	120.0	100.0
130	10180.0	10175.0	612.0	598.1	11105.0	808.0	130.0	105.0
170	10207.5	10200.0	703.0	684.6	11120.0	790.0	145.0	117.5
210	10265.0	10250.0	801.0	753.3	11140.0	770.0	155.0	125.0
250	10312.5	10300.0	855.0	829.9	11170.0	750.0	170.0	125.0
295	10380.0	10375.0	954.8	915.3	11210.0	730.0	180.0	125.0

to fit the data of Kirmaier and Holten in the low energy region of the spectrum. The resultant parameter sets arising from the lineshape simulations are collected in Table III. Fits to circular dichroism data were used to constrain the position of the upper exciton component at higher temperatures, where the shoulder visible at 4 K is obscured. This leads to some uncertainty in the results, because the CD measurements were not carried out on the same samples as the absorption. These experiments clearly need to be redone utilizing PVA films.

With this caveat, the results of the simulations support the thermal expansion model described above. Not only do the parameters move in the right direction, but their functional forms are nearly identical, suggesting that all depend upon a single physical quantity (postulated to be the intermolecular SP excited state equilibrium distance). Note that the only remaining temperature-dependent parameter, the damping constant (γ in Table III), has a quite different behavior, changing at low temperature and saturating at room temperature. This is just the form that is expected if the damping is controlled primarily by acoustic phonons.

The electronic structure calculations of Fajer and co-workers [41] (discussed in subsection III-A.2) also fit in well with the thermal expansion picture. The sensitivity of the SP optical spectrum in these calculations to the intermolecular separation suggests that this parameter is capable of yielding the strong effects observed experimentally, in accord with the hypotheses made above.

IV-B. Stark effect spectroscopy

Stark effect measurements on the RC were initiated by Feher and co-workers several years ago [94]. These workers observed that the P* band displayed an anomalously large Stark effect as compared to other RC pigments and to monomeric Chl and BChl molecules in solution. The direct interpretation of this result is that the magnitude of the difference in the dipole moment of the P* state as compared to the ground state is substantially larger than the difference for analogous monomer excitations. If one assumes that there is nothing unusual about the SP ground state, the logical conclusion is that the excited state possesses an unusually large dipole moment.

Careful quantitative experiments were then carried out by Lockhart and Boxer [87,133], who also obtained data as a function of the angle between the applied electric field and a polarized light souce (accurate measurements were also subsequently made by the Feher group [95]; the work of the two laboratories is in good agreement). By fitting this data to a standard functional form, they were able to extract the angle between the optical transition dipole moment and difference dipole moment of the P* band. The angle, 38.5°, is quite different from that obtained for a monomer; it is difficult to draw unambiguous conclusions beyond this observation. This group has also recently investigated the Stark effect observed from fluorescence of the SP [88,125]. A predominantly zeroth derivative (as opposed to the usual second derivative) lineshape is obtained, which the authors interpret as being due to effects of the electric field upon the decay of P* (i.e., on electron transfer from P* to P^+H^-).

The most straightforward explanation for the absorption Stark results is that some charge transfer (CT) character is mixed into the P* band. There are various ways in which this could occur, as will be discussed in detail in subsection IV-D. Quantitative analysis of the fluorescence data, extracting a second derivative component, suggests that the difference dipole does not increase as function of time; this implies that the CT character is created instantaneously when one excites the P* band.

IV-C. Photochemical holeburning measurements

Several research groups have now carried out photochemical holeburning experiments on the P* band of the RCs of viridis and sphaeroides [96–98]. In these experiments, the sample is first irradiated with a 'burn' laser, which drives some fraction of the SP molecules into their excited state (P*) which rapidly decays via the usual charge separation process to P^+H^-. A probe laser then interrogates the residual distribution of ground state molecules. If the sample is homogeneously broadened, then each RC is equivalent to every other one, and one would expect to see the absorption band decrease uniformly in intensity. On the other hand, if there is substantial inhomogeneous broadening, a 'hole' will be burned in the spectrum at site energies which the burn laser preferentially excites. For a typical molecule embedded in a crystalline solid or a glass at cryogenic temperatures, at least one sharp hole, corresponding to the zero-phonon line (ZPL) of the homogeneous spectrum, will appear. Sharp side holes or broad phonon side-bands can also often be detected.

For porphyrins in glasses [99] or chlorophyll inserted into myoglobin [100], holeburning experiments yield results in accord with these expectations. In particular, a sharp (less than 1 cm^{-1}) zero-phonon hole is readily observed. This indicates that there is nothing about an isolated chlorophyll monomer or a genetic protein environment that would lead to an alternate result. The initial observations for the P* band of the reaction center, however, did not display a sharp zero-phonon hole at all; instead, broad holes of a width of roughly 95% of the full width of the band were observed.

Recent experiments by Tang et al. [103] have revealed a weak ZPL when one excites at specific energies

within the absorption band. This feature, which appears to have a roughly 10 cm^{-1} width, is most easily observable when one prepares RCs in a glycerol/water glass, as opposed to PVA films, presumably because the inhomogeneous broadening is smaller. Additionally, one can detect a very broad 0-1 vibrational side hole 120 cm^{-1} from the ZPL. However, a sharp side hole cannot be observed (despite the large amplitude of the 0-1 feature), indicating that there is unusually strong dephasing of some type which must be explained.

Prior to these recent experiments, two types of explanations for the absence of the ZPL has been proposed. The most detailed treatments of each are, respectively, that of Hayes and Small (HS) [73,74] and of Won and Friesner (WF) [69,70]. We will focus on these papers in the interest of clarifying the similarities and differences between the two models, while noting that other workers have also advocated ideas along the same lines.

In HS, the disappearance of the ZPL is attributed to a large exciton-phonon coupling constant, presumably for the low frequency intermolecular mode of the SP which one would expect to be strongly coupled to the optical transition. The numerical values originally utilized by HS for their single mode model were $\omega = 30$ cm^{-1} and the Huang-Rhys factor of the mode, $S = 8$. The numbers were obtained from attempts to fit the temperature dependence of the P* band using a harmonic form for the excited state potential [72].

As discussed above, the thermal expansion model appears to yield a more satisfactory explanation of the temperature dependence than a harmonic model. In this case, a frequency of 50 to approx. 100 cm^{-1} and an S of 1–2 are obtained at 4 K. This value of S is not large enough to completely destroy the ZPL. In this picture, a different effect must therefore be invoked to explain the experimental results.

In WF, the absence of the ZPL is explained by coupling of the P* vibronic manifold to a nearby charge transfer state. Mixing of the two electronic configurations causes a chaotic redistribution of oscillator strength from the ZPL to a dense manifold of states, much a occurs in highly excited vibrational states of molecules in the gas phase [101]. In the latter case, the chaotic spectrum is due to anharmonic coupling between the molecular vibrational modes. In the present situation, a similar effect is achieved because the coupled two electronic state system is effectively 'anharmonic', this behavior has been noted previously in model studies of two electronic states coupled to a set of vibrational modes [102]. This model requires that the electronic coupling strength and CT-P* energy gap both be on the order of the bandwidth of the P* transition, i.e., in an intermediate coupling regime. In the WF model of charge separation, this specific form of the coupling plays a central role in enhancing the initial

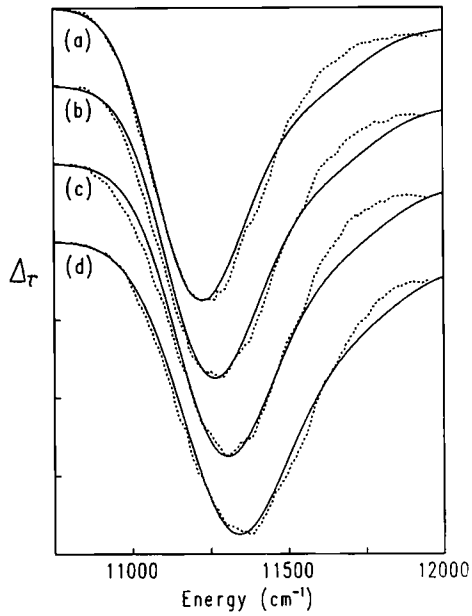

Fig. 6. Hole spectra of the *Rb. sphaeroides* RC are compared to the experimental data (dotted lines) measured at 1.5 K [96]. Burn laser frequencies are (a) $\omega_L = 11{,}180$ cm^{-1}, (b) $\omega_L = 11{,}253$ cm^{-1}, (c) $\omega_L = 11{,}345$ cm^{-1} (d) $\omega_L = 11{,}470$ cm^{-1}.

charge separation without contribution to the efficiency of the back reaction to the ground state.

Both the WF and HS models were able to provide a semiquantitative description of the older experimental results. Fig. 6 displays the simulated hole spectra as a function of burn wavelength for *Rb. sphaeroides*. The parameter set is identical to that used for simulating the other optical properties. Note that the wavelength dependence emerges from the model without explicit parameter adjustment. However, this can also be accomplished in the HS model, so this observations.

The crucial question revolves around the proper description of how the P* state acquires CT character. If one can consider the P* band as arising from a single electronic state, then the HS description is plausible, although still not entirely without problems (e.g., even if the ZPL is destroyed, specific additional conditions are required so that one does not observe sharp side holes). The WF theory explicity argues that one has to consider two underlying coupled electronic states in analyzing the P* band. In the next section, we investigate the internal consistency of each of these viewpoint.

The new experiments described above can be thought of as more effectively removing the inhomogeneous broadening than the earlier work, to reveal some underlying structure. One consequence of these experiments is that the strongly coupled low frequency dimer mode hypothesized in both treatments can be directly observed, and the frequency and Huang-Rhys factor explicity evaluated. The values are in fact quite close to those proposed by WF ($S \approx 2$), indicating that the analysis of the temperature dependence leading to the

much larger values ($S \approx 8$) is incorrect. Additionally, these experiments identify the shoulder that is sometimes seen on the red edge of the P* band as the 0-0 origin of the dimer mode progression; this explanation was suggested by WF several years ago [132].

One is still left with the question of the weakness of the ZPL and the absence of sharp side holes. In their most recent work, Small and coworkers explain these observations by invoking phonon broadening [103]. However, given the strength of the dimer mode and its relatively large spacing, one would normally expect to see at least a sharp 0-1 side hole. Suitable adjustment of parameters in the WF model (in particular, reduction of the electronic coupling to the CT state or increasing the energy gap between the CT and Q_y states) will leave a weak ZPL while eliminating any subsequent sharp features. Spectra of this type are displayed in Figs. 3–6 of Ref. 69.

One cannot, of course, choose between these two explanations on the basis of the holeburning experiments alone. Instead, one has to consider the entire set of experiments carried out on the RC. As will be seen below, the attractiveness of the WF proposal is the simultaneous rationalization of other unusual phenomena, which are entirely unrelated to the hypothesis of strong phonon-induced dephasing. Thus, while the latter model would be more likely in a conventional chemical physics context (on the grounds that it requires a less specific assumption), there are strong independent reasons to believe that a second nearby electronic state is important in the present case.

IV-D. Charge transfer character of the P band*

As we have seen from previous discussions of the Stark effect and holeburning results, most workers agree that the P* state has some CT character. The question is how CT configurations interact with the Q_y configurations of the SP to produce this result. This question has important implications for the mechanism of charge separation, as will be discussed in subsection V-B.

A reasonable way to examine this question is to begin with a set of Q_y and CT many-electron basis states, specify their diagonal energies and off-diagonal couplins, and allow them to mix via configuration interaction. In a purely electronic model, this is done by simply diagonalizing the resulting interaction matrix, yielding a new set of eigenstates which are linear combinations of the old zeroth-order basis functions.

In an ab initio electronic structure calculation, the CI matrix elements would be generated from a rigorous (albeit limited) approximation to the true Hamiltonian of the system. In the semiempirical studies of the RC carried out to date, the matrix elements are estimated by means of heuristic, uncontrolled approximations [39,42,43]. This is particularly problematic for the CT states, which are not easy to study experimentally (because of their intrinsically low oscillator strength) and which are undoubtedly influenced substantially by the protein environment. We will therefore adopt the point of view of examining the consequences of making different types of assumption concerning CI with CT states, asking what sort of experimental predictions result from various types of qualitatively different parameters sets.

To investigate the P* band in this context, we consider a very simple 3×3 CI matrix. The three states are the Q_y states of the two SP monomers and a single internal CT configuration of the dimer. The assumption here is that only one of the two possible dimer CT states lie close in energy to the Q_y states, having been shifted there via interactions with the protein. This assumption is consistent with most of the semiempirical calculations to date; indeed, a 3×3 model equivalent to that just described can be extracted in straightforward fashion from the larger matrices typically treated in these calculations without altering the results significantly. The CT state is assigned zero oscillator strength, which is consistent with both calculations and the experimental polarization of the P* band [85] (which indicates that its allowed character derives entirely from the SP Q_y transitions).

The two SP states interact and split to form the upper and lower dimer components. We must then consider the interaction of these two states with a CT state. First, suppose that the interaction of the CT state with the SP Q_y states is very large (about 1000 cm^{-1}), as has been proposed in several papers – the critical feature is that it is larger than the bandwidth of the P* state (400 cm^{-1}) and larger than or comparable to the splitting of the diagonal energies of the CT and Q_y states. In this case, there will be a substantial admixture of the CT state with the dimer states, in agreement with the Stark measurements. Parson and Warshel have also suggested that the interaction repels the lower dimer state, thus accounting for some fraction of the red shift of the P* band [38,104].

Unfortunately, this picture has another consequence which is not in agreement with experiment. Under the conditions described above, it is impossible to avoid the generation of three new electronic states, each with substantial oscillator strength. (The reader can convince him- or herself of this by diagonalizing 3×3 matrices with the appropriate properties and examining the resulting eigenvectors.) Two of these states are observed experimentally, e.g., in *viridis* at 850 and 990 nm. Where, however, is the third (high energy) state, predicted by this model to have both oscillator strength and CT character? In the PW calculations, for example, the transition in question lies at 670 nm and has a dipole strength of 10.2 D^2 [38], which is larger than that of the

Q_x transitions of the SP that are readily observable in this region. Furthermore, no anomalous Stark effect has been found at high energies. While it is possible to rationalize these negative results by ad hoc arguments (e.g., that the state is, for some reason, extremely broad), this seems unconvincing. At the very least, these proposals have a serious problem to address.

The alternative is to hypothesize that the CT transition interacts with the P* state via an intermediate value of the electronic coupling (about 100 cm^{-1}) and that they are close enough in energy to produce a substantial admixture. In the simplest picture, the 'new' state is buried under the P* band. This hypothesis is consistent with the WF picture of the holeburning experiments [69,70], as well as presenting no difficulties of the type described above. Other supporting evidence will be presented in Section V.

One objection to this construction has been proposed by Fischer and co-workers [105]. They argue that if the P* band had two underlying states, this would be reflected in the lineshape of the Stark spectrum, which would display a first (rather than second) derivative character. It is not clear if this is the case, however, if the two states in question are reasonably close in energy, are substantially broadened by inhomogeneous distributions and acoustic phonons, and are coupled to a vibronic manifold which introduces further smearing out of the individual character of the electronic states via phonon exchange. All of the above effects are evident in the large width of the P* band and the holeburning spectrum. Nevertheless, this argument needs to be carefully investigated by explicit simulation of the Stark lineshape of the P* band for model Hamiltonians of the type proposed by WF. Such calculations are currently in progress in our laboratory.

From an experimental point of view, a useful measurement to determine the underlying electronic nature of the P* state would be a resonance Raman study in which excitation was tuned through the P* band. If there are two electronic states under this band, one would expect to see some evidence of B term scattering in the excitation profiles. In addition, the coupled vibrational modes (e.g., the low frequency intermolecular mode of the SP discussed above) could be directly determined, and the magnitudes and temperature dependence of the Franck-Condon factors obtained.

There are additional complexities which must be considered in constructing a genuinely quantitative theoretical model of the P* state. For example, the interaction of the CT state may be different for the upper and lower exciton components. It is possible that such refined models could be differentiated by their ability to reproduce the details of the experimental spectra (e.g., the Stark lineshape). This sort of analysis may become feasible when the basic qualitative observations are well understood.

V. Electron transfer dynamics

V-A. Transient absorption measurements of primary charge separation

The most direct approach to studying charge separation in the RC is time-resolved absorption spectroscopy. Typically, an initial pulse excites some chromophore in the RC, which transfers its energy to the SP in less than 100 fs [22–24] (it is also possible to directly excite the P* band). A probe pulse then monitors the time-dependent absorption spectrum of the RC at a series of delay times after the initial pulse. In this process, one can either obtain the entire absorption spectrum (by making the probe pulse a white light continuum) or observe at selected wavelengths.

In principle, the analysis of such a measurement is straightforward; the observed spectrum reflects bleaching of components that are converted to a differing form, and enhancement of the spectral characteristics of the new species. In practice, it is not always easy to determine what the new spectra should look like, particularly when there are numerous overlapping bands and when some of the actual or hypothesized species cannot be observed under controlled circumstances.

We will first discuss ultrafast experiments that probe the initial charge separation from P* to P^+H^-. Measurements by several groups with subpicosecond time resolution have established the rate of disappearance of P* and appearance of P^+H^- to be on the order of 3 ps at room temperature [22–24,119–121]. A complete set of temperature dependent rates for both *viridis* and *sphaeroides* has recently been produced by Fleming et al. [19,20]. The rates are similar at low temperature but differ by a factor of two at room temperature.

A major focus of the subpicosecond kinetics measurements was an attempt to detect the appearance of B^- as an intermediate. The obvious approach is to look for bleaching of B; this is complicated by the fact that the B absorption peak is subject to an electrochromic shift induced in the charge separated state P^+H^- (readily observable after charge separation has taken place). Fleming et al. constructed a kinetic model in which a 'rigid band shift' (i.e., only the peak position of the B absorption was altered) was assumed and were able to fit the spectral changes at several wavelengths quite accurately assuming no participation of B as a detectable intermediate [19,20]. Indeed, alternative models with B as an intermediate were acceptable only if the rate of transfer from B to H was assumed to be more than 50-times faster than that from P to b, thus implying an ET rate of less than 20 fs for the former step. Kirmaier and Holten have reached similar conclusions from experiments on *Rb. capsulatus* (an ET rate differential of a factor of 20 between the two steps was obtained) by a somewhat different method of data analysis [120].

A final point of importance is that, within experimental error, no immediate bleaching of B is observed upon photoexcitation of the SP. This argues against attributing the CT character of the P* band to the state P^+B^-, because if there was strong mixing of any state of B into P*, one would expect a significant initial bleaching of B. The internal CT state thus appears to be responsible for the CT contribution of P* by default. Further evidence along these lines comes from a site-directed mutagenesis experiment, which will be discussed in Section V-C.1.

V-B. Theoretical models for the primary process

The transient absorption data provide first-order constraints in constructing theoretical models of primary charge separation. For example, one can probably rule out a direct mechanism in which B plays no role at all; the electronic coupling of P and H is, according to all estimates to date, not large enough to generate a rate significantly less than 100 ps. Of the remaining possibilities, none can be definitively eliminated at this point, although some face more difficulties than others. Following is a list of proposed mechanisms:

(1) ET from P to H is mediated by superexchange coupling through B [65,66]. This implies that P^+B^- is higher in energy than P*. It requires fairly large off-diagonal electronic coupling matrix elements between the participating electronic configurations, in contrast to the explicit intermediate hypothesis. The failure to detect bleaching of B is here completely straightforward.

(2) B participates as an explicit intermediate [60–63]. As discussed above, this raises difficulties with regard to the detectability of B in the transient absorption experiments. Several suggestions as to how these difficulties might be overcome have been made, and will be presented below.

(3) The state B^+H^- is created right after optical formation of P*, followed by hole and electron transfer to generate P^+H^- [39,43]. This mechanism also has problems in explaining the failure to observe bleaching of B. As it is analogous in this respect to the simpler model (2), and as no specific experimental evidence has been produced to show that it is more likely than (2), we shall not pursue discussions of this model further; interested readers should consult Ref. 43.

In addition to specifying which of these mechanisms is correct, the task of giving an appropriate description of each elementary step of the electron transfer dynamics is still not completed. One possibility is that standard nonadiabatic multiphonen theory is adequate to describe all relevant ET steps in the primary process. However, the rate of individual steps in various proposed mechanisms is such that some steps could be adiabatic. In what follows, we begin by investigating the two basic proposals (superexchange, explicit intermediate) in some detail. We then discuss some of the more global questions concerning the ET dynamics raised above.

In providing references for the various charge separation mechanisms, we have not attempted to be exhaustive or to establish priority. Rather, we have indicated several relatively recent papers in each category which contain substantive discussions of the mechanism in question. Earlier proposals suggesting most of the mechanisms in some form can be found in the literature.

V-B.1. Superexchange model

We first give a brief presentation of the simplest form of the superexchange model, following the treatment of Marcus [61]. We will assume here that the one-step process mediated by superexchange is nonadiabatic (weak electronic coupling), so that the rate is proportional to V_{eff}^2, where V_{eff} is the effective matrix element coupling P* and P^+H^- incorporating the effects of the intermediate state P^+B^-. If one makes reasonable assumptions, a value of V_{eff} of around 20 cm^{-1} is required to yield a rate constant in agreement with experiment.

The effective matrix element is readily calculated via perturbation theory, assuming that the intermediate state is significantly higher in energy than the acceptor state. Labeling the donor (P*) to be state 1, P^+B^- to be state 1, P^+B^- to be state 2, and P^+H^- to be state 3, we have

$$V_{\text{eff}} = \frac{H_{12}H_{23}}{H_{22}(Q) - H_{33}(Q)} \tag{1}$$

where Q represents the entire nuclear potential surface, H_{ij} is the exchange coupling of state i and j, and $H_{ii}(Q)$ is the energy of the state i at nuclear configuration Q. The matrix elements must all be evaluated at the crossing point of the potential surfaces of states 1 and 3. The normal assumption is that the off-diagonal terms are weak functions of the nuclear potential surface (Condon approximation), whereas the diagonal terms can vary significantly. By positing relative values of H_{12} as compared to H_{23} (based on, for example, electronic structure calculations), one can then, by estimating the diagonal terms in Eqn. 1, extract the value of H_{12} required to achieve the experimental ET rate. Values obtained range between 70 and 140 cm^{-1}, with one result in between.

These numbers are larger than some estimates based on semiempirical electronic structure calculations [38,42,106]. More seriously, a significant discrepancy with experiment was also demonstrated by Marcus. One can carry out a similar analysis and predict the singlet-triplet splitting of the radical pair P^+H^-, which de-

pends upon the same set of coupling matrix elements as does the ET rate (although they are to be evaluated at the equilibrium geometry of P^+H^- rather than at the crossing point); the relevant formulas are:

$$E^S - E^T \approx \frac{V_{eff}^2 (H_{11}^S - H_{11}^T)}{(H_{11}^S - H_{33})(H_{11}^T - H_{33})} \quad (2)$$

where the ST splitting of P*, $(H_{11}^S - H_{11}^T)$, is known to be 0.4 eV [107,124], and that of the charge separated species are taken to be negligible by comparison, as the dipolar couplings in these configurations are surely much smaller than in P*.

If one substitutes in the values obtained for H_{12} and H_{23} above, an ST splitting two to three orders of magnitude larger than the experimentally observed value of $2 \cdot 10^{-7}$ eV [16] is obtained. To express the argument in simple physical terms: rapid ET via superexchange requires relatively large off-diagonal coupling matrix elements. These matrix elements should then transmit the ST splitting of P* to P^+H^- much more effectively than they apparently do. Thus, it appears as though the superexchange mechanism leads to serious disagreement with experiment.

A way out of this dilemma has recently been proposed by Won and Friesner [67]. These authors incorporate the internal dimer CT state (discussed at length in subsection IV-D, above) into the superexchange model. The key point is that this state will have a small ST splitting, because the unpaired electrons of the triplet are at different monomers. If most of the superexchange coupling occurs through this state (plausible, as its ionic character would lead to orbital relaxation facilitating better overlap with P^+B^-), then the ST splitting of P^+H^- can be sufficiently small to agree with experiment. Fig. 7d and c display the effective coupling between P* and P^+H^- as a function of coupling between P_{CT} and P^+B^- assuming a reasonable set of other model parameters (see Ref. 67 for details) as well as the ST splitting of P^+H^- for the same model. These are to be contrasted with the analogous effects of raising the direct coupling between P* and P^+B^-, shown in Fig. 7b and a, respectively.

The above result can be understood in simple terms as follows. The original superexchange model contains three triplet and three singlet states; the WF model additionally incorporates both a P_{CT} singlet and triplet state. The singlet state is assumed to lie close in energy to the singlet P* state (a number of values are examined in Ref. 67, e.g., 100 cm^{-1}); the triplet state is taken to lie at a similar (within 50 cm^{-1}) energy, for the reason given above (relatively large separation of the unpaired electrons). Because the energy splitting of the two states is so small, they each perturb the corresponding radical-pair spin states in a nearly identical fashion; thus, a negligible splitting results from this perturbation

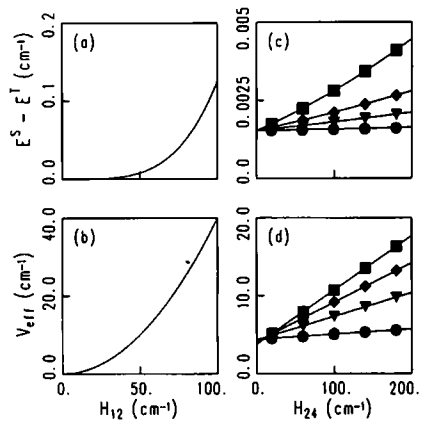

Fig. 7. (a) The S-T splitting, $E^S - E^T$, and (b) the superexchange matrix element V_{eff} as a function of H_{12}. The P_{CT} state is decoupled, i.e., $H_{14} = H_{24} = 0.0$ cm^{-1}. $H_{23} = 2H_{12}$, $\Delta E(^1P^* - {}^1P^+B^-) = 500$ cm^{-1}, $\Delta E(^1P^* - {}^1P^+H^-) = 1500$ cm^{-1}, and $\Delta E(^1P^* - {}^3P^*) = 3200$ cm^{-1}. (c) The S-T splitting, $E^S - E^T$, and (d) the superexchange matrix element V_{eff} as a function of H_{24} for various CT coupling H_{14}; *l*, 10 cm^{-1}; *t*, 50 cm^{-1}; *u*, 100 cm^{-1}; *n*, 200 cm^{-1}. The CT state is coupled with P*; $\Delta E(P_{CT} - {}^1P^*) = 100.0$ cm^{-1}, and $\Delta E(^1P_{CT} - {}^3P_{CT}) = 0$ cm^{-1}. All other parameters are identical to those used in (a) and (b) except that H_{12} is set to 33 cm^{-1}.

through the superexchange pathway. The effective coupling of P_{CT} to P^+H^- can thus be increased substantially (to generate an adequate electron transfer rate) without leading to a contradiction with the magnetic field experiments. Qualitatively, this conclusion is not sensitive to precise parameter values, although an acceptable range of parameter validity has not been delineated.

In the above picture, the state P_{CT} acts as a trigger for charge separation, linking the excited electronic state P* with the superexchange pathway. A crucial point is that this trigger is not available for recombination from P^+H^- to the ground state, because its participation in forward transfer is due to an intermediate (but quasiresonant) coupling with P*. If the coupling of P_{CT} with P* were very strong (as has been proposed in other models [38,89]), it might well facilitate coupling of P^+B^- to the ground state as well. Note that a typical result in synthetic model systems is that if one makes the electronic coupling to intermediate states very strong, recombination to the ground state is quite rapid. The suggestion here is that the reaction center is optimized by tuning the coupling and energetics of the superexchange pathway so that it is accessible in only the forward direction, and the the primary means of accomplishing this is adjustment of the matrix elements and energy of P_{CT}.

A different explanation of the small singlet-triplet splitting has been suggested by Michel-Beyerle, Jortner and co-workers [65,66,108]. They assume that P* consists of only one electronic state, (in contrast to WF), and explain the enhanced efficacy of superexchange coupling for ET (as compared to ST splitting) by posit-

ing a conformational change in the protein upon transfer of an electron, so that the relaxed P^+H^- state has a much weaker coupling than does the configuration which carries out ET. Some support for this has been obtained from molecular dynamics simulations of Treutlein et al. (see subsection III-B.1) in which confirmational alterations were along these lines were reported [56,57]. However, the fact that charge separation appears to function in a more or less identical fashion at cryogenic and room temperatures suggests that one ought to be cautious in hypothesizing a critical role for such conformational changes in the primary process.

V-B.2. B as an explicit intermediate

Several attempts have been made to rehabilitate the explicit intermediate mechanism from the difficulties posed by the transient absorption results described above. One possibility has been noted by Marcus, namely that the second step ($P^+B^- \rightarrow P^+H^-$) could be adiabatic, thus explaining its ultrashort lifetime [62,63]. Almeida and Marcus have carried out model quantum mechanical wavepacket calculations to demonstrate the plausibility of this hypothesis (Marcus, R.A., personal communication). Another way of looking at this is to assume that P^+B^- and P^+H^- are so strongly coupled that the initial transfer is to a delocalized state of these two species, which rapidly relaxes to the lower energy configuration, P^+H^-.

A second possible explanation has come out of the molecular dynamics simulations of Warshel and coworkers [55]. These authors use a semiclassical ET theory developed by Hwang and Warshel [109], in which the energy gaps between the various configurations are allowed to fluctuate in time, and the final rate constant is obtained by integrating over these fluctuations. Both superexchange and explicit intermediate models were investigated.

The off-diagonal electronic coupling matrix elements obtained by Warshel et al. in their QCFF-PI calculations are rather small; hence, they experienced difficulties in extracting a sufficiently large rate constant for ET in the superexchange mechanism. They therefore favored the explicit intermediate mechanism, asserting that the energy fluctuations result in a small concentration of the P^+B^- intermediate which is below the limits of detectability of Refs. 22–24. This proposal is an interesting idea, and views the problem in a somewhat different manner than previously described theoretical treatments. It does appear to rely upon a rather specific tuning of various coupling and energetic parameters, as well as many details of the protein model. As none of these can be considered completely reliable, and as the theoretical electron transfer methodology itself contains a number of approximations, a more qualitative prediction of this model which could be tested experimentally would be desirable.

V-C. Other dynamical experiments relating to primary charge separation

Having presented the basic arguments for and against the existing primary charge separation models, we now consider additional experiments which bear directly upon these models. These include investigations of proteins modified by site directed mutagenesis and application of a strong electric field across oriented RCs. Both of these areas are expected to provide a great deal of crucial information as the techniques become more refined and widely used.

V-C.1. Site-directed mutagenesis of the RC of Rb. capsulatus

The initial RC system which has been extensively subjected to genetic modification is that of the bacterium *Rb. capsulatus*, via the pioneering efforts of Youvan and coworkers [11–13]. This RC has not yet been crystallized, although its amino-acid sequence is known; it was selected primarily because a previous history of genetic manipulation has been well established. The sequence is sufficiently homologous to *sphaeroides* and *viridis*, however, that important residues can be selected for mutation in a systematic fashion based upon the crystal structures of the latter species.

Of the various mutants have been prepared, some have yielded surprising negative results. For example, residue Glu^{L104} forms a hydrogen bond with a carbonyl group on H_L; no analogous residue exists on H_M. It was thought that this residue would be important in stabilizing charge separation on the L branch. When Glu^{L104} is changed to Leu, however, there is little change in the rate or efficiency of primary charge separation [13,118]. On the other hand, the Q_x absorption spectrum of H_L shifts so as to be close to that of H_M (a similar, but less pronounced, phenomenon occurs in the Q_y region), demonstrating that the hydrogen bond is responsible in large part for the splitting of the pheophytin bands in the optical spectrum.

From the standpoint of the primary charge separation mechanism, the most important mutant prepared to date is one in which His^{M200} is changed to Leu [12]. The resultant organism is able to carry out charge separation, although the quantum yield is reduced to roughly 50% [14]; the organism does not grow photosynthetically, for reasons that are not yet well understood [12]. Careful analysis of the optical spectrum (shown in Fig. 8, along with the wild-type spectrum for comparison) and other experiments suggests that the effect of the mutation is to pheophytinize one of the SP molecules, yielding a heterodimer as a SP. Transient kinetics indicate that the rate of primary charge separation is reduced by approximately one order of magnitude [14,134] as compared to wild-type organisms.

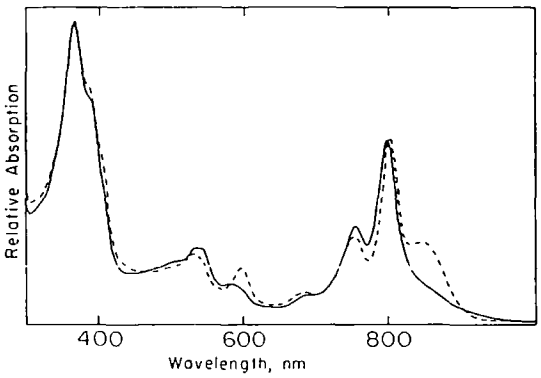

Fig. 8. Comparison of the room temperature absorption spectra of RCs from the $His^{M200} \rightarrow$ Leu mutant (solid line) and wild-type (dashed line) *Rb. capsulatus*. Obtained from Ref. 14.

An extremely interesting observation is the appearance of a pheophytin anion spectrum at roughly 600 fs (this estimate is, in fact, instrument-limited) after initial excitation of the RC [14,134]. This band cannot be due to H_L, because the absorption spectrum of that molecule has not yet been bleached at such short times. The simplest interpretation is that an internal charge-separated state of the heterodimer, $BChl^+BPh^-$, has been formed, as an intermediate, and that charge separation proceeds out of this state. If correct, these results provide support for the WV 'trigger' model of primary charge separation. The argument is that the internal CT state of the heterodimer is just the P_{CT} state hypothesized in the WF model, shifted down in energy by roughly 0.2 eV (the difference in energy between a BChl and BPh anion in solution [117]). The reduced quantum yield of the modified RC is, possibly, explained in this picture by an alteration of the thermodynamics of charge separation, in that the internal CT state now lies at lower energy than previously and hence may contain a larger fraction of the occupation probability than in the native system when a quasiequilibrium is reached. The population residing in this state would decay via radiationless processes to the ground state, as suggested in Refs. 14 and 134.

Further support for this picture comes from recent Stark effect measurements on the heterodimer by Norris and co-workers [122]. While the observations are not trivial to interpret, the simplest analysis indicates that there are now two states in the near-infrared region. In particular, the long, very weak tail that can be seen at low energies in the absorption spectrum displays a very large Stark amplitude, suggesting that it arises from the internal CT state, which vibronically borrows intensity from the Q_y state of the remaining BChl of the SP. The zeroth order electronic energy of the CT state can be placed below the furthest extent of this tail, as upper vibrational levels are the ones likely to mix efficiently with the (now) higher-lying Q_y transition. Additional recent work of importance is that of Breton et al. (personal communication), who carried out linear dichroism experiments on the heterodimer which indicate that the pigment orientations are very similar to those in the wild-type organism. This suggests that pheophytinization is the only significant alteration of the system that needs to be considered (as has been assumed in the foregoing discussion).

More experiments and theoretical analysis will be required before the above conclusions can be definitively confirmed. It is clear, however, that site-directed mutagenesis experiments will have an increasingly important role to play in unraveling the working of the RC in the years to come. For example, the question of which (if any) protein residues stabilize the internal dimer CT state can be readily addressed by this technique, once a target set of residues are proposed.

V-C.2. Electric field experiments on oriented RCs

Feher and co-workers [110] and Dutton and co-workers [111,112] have developed techniques to prepare oriented films of RCs for carrying out electric field measurements. The Dutton group uses Langmuir-Blodgett films and has developed specialized methodology for studying these films under the application of high electric fields (150 mV/nm) and in an electrochemical cell. Current efforts are aimed at carrying out fast transient spectroscopy under high-field conditions.

The hypothesis is that the field shifts the energy levels of the participating electronic configurations in proportion to the dipole moment of the configuration; thus, species with the highest degree of spatial charge separation will be most affected (orientation of the dipole also plays a role). There are several potentially complicating factors in this analysis. (1) Off-diagonal matrix elements may be affected as well. In a superexchange mechanism, one can certainly affect the effective coupling by changing the energy of the virtual intermediate. (2) An accurate calculation of the energy shift involves estimating local field corrections due to the polarizability of the protein medium. (3) One must fit measurements in the context of a charge separation model; it is not clear how easy it is to distinguish the different models on the basis of the experimental results (on can, after all, adjust the parameters of each model to achieve a best fit).

Popovic et al. have recently shown that application of an electric field gradient of 120 mV/nm along the direction of charge separation (i.e., so as to lower the energy of P^+H^-) leads to a decrease in the quantum yield of P^+H^- formation to about 0.75 from a value of 0.96 at zero applied field [112]. They have interpreted this as an effect on the rate of primary charge separation; note that this inference is not unambiguous, as one could in principle produce a similar phenomenological result by altering the rate of recombination to the ground state. The former hypothesis does seem

more likely, on the basis of the order of magnitude of variation required to produce an effect of the magnitude observed.

Dutton and co-workers fit the electric field dependence of their measurements to several charge separation models [113]. They were unable to rule out any of them, with the exception of a simple Marcus reaction in which $\Delta G = \lambda$. As will be discussed below, this commonly drawn inference (from the lack of temperature dependence at low temperature) for biological systems appears to be rather questionable in the reaction center.

Bixon and Jortner have recently provided a more detailed theoretical treatment of the expected electric field dependence of observables under a variety of conditions and assumptions [114]. They make several predictions of results of new experiments depending on the the model assumed for primary charge separation. For example, if the sequential mechanism is correct, the P^+B^- intermediate should be observable in a kinetic experiment with oriented RCs at large negative fields. One can also distinguish the sequential mechanism from the superexchange model based on the quantitative analysis of low field fluorescence quantum yields measured with unoriented RCs.

If a substantial effect of the electric field can be seen in fast transient absorption experiments (as opposed to the less direct fluorescence measurements carried out to date), it may provide qualitatively important new information. For example, one might hope to lower the energy of the putative P^+B^- superexchange intermediate below that of P*. Much depends upon whether the quantitative parameter values are such that these effects will be readily observable.

V-C.3. Temperature and free energy dependence of ET reactions in the RC

We have said very little to date concerning the other reactions involved in the initial stages of charge separation; these include various back reactions and the forward transfer from H to the quinone Q_A. These reactions are not ultrafast over an exceptionally long distance, so they do not present the same sort of puzzle that the primary forward reaction does. They do, on the other hand, display an unusual behavior with regard to their temperature and free energy dependence. This behavior may be relevant to the primary reaction as well, and may also possess some very general implications for ET in certain types of protein environments.

Gunner et al. have carried out a series of experiments in which they systematically replaced the ubiquinone which consistutes Q_A in the natural system with more than 50 modified quinone derivatives [115]. This allows systematic variation of the free energy of the donor in the back reaction $Q \rightarrow$ ground state and of the acceptor in the $H \rightarrow Q$ reaction, while presumably preserving the value of the reorganization energy and of the electronic coupling matrix element to a rough approximation. These studies were carried out at a series of temperatures ranging from 4 K to 300 K.

An attempt to fit the resulting two-dimensional (ΔG, T) data set to a classical Marcus expression failed unambiguously. A more succesful fit was achieved by utilizing nonadiabatic multiphonon theory and assuming two active vibrations, one at low frequency (120 cm^{-1}), and one at high frequency (1600 cm^{-1}) [116]. It is clear that the latter theory could yield equally good fits if many more modes were utilized; such a distribution of frequencies is not unlikely in view of the complexity of the environment and of the porphyrin chromophores.

The crucial observation, however, is that below 100 K no temperature dependence was observed, regardless of the value of ΔG. This provides irrefutable evidence against the claim that such an observation implies that $\Delta G = \lambda$, where λ is the reorganization energy (which has often been made with regard to ET reactions in the RC), or even the less strong claim that this relation holds approximately. In the experiments of Gunner et al., ΔG was varied by more than an electron volt without the slightest effect on the flat temperature dependence in the 4–100 K region; obviously, ΔG cannot be 'close' to λ for each of these experiments, by any reasonable definition of proximity.

On the other hand, the data are trivially explained if one simply assumes (as is concluded in Ref. 116) that coupling to low frequency protein modes (those of frequency less than 70 cm^{-1}, and hence capable of activation below 100 K) is very weak. This assumption also is in concordance with what one might expect in a frozen glass (which a protein at these temperatures resembles strongly); the dipolar reorientations which readily occur in a room temperature polar liquid are hindered and/or frozen out. Additionally, the degree of polar character in the RC is not great to begin with, so that this picture may be correct even at room temperature.

It is interesting to note that the primary reaction (and other reactions in the RC as well; see, e.g., Refs. 25 and 91) exhibits this same feature in its temperature dependence; one might therefore guess that it has the same origin (although supporting ΔG studies are not now available to demonstrate this unambiguously). Here, however, the energy gap is sufficiently small (0.17 eV) that assertions that ΔG is close to λ are not completely unreasonable (although the reasoning used to draw the conclusion is just as flawed as in the previous case). On the other hand, the temperature dependence above 100 K may well be due to thermal expansion of the SP, as discussed in subsection IV-A; at this point, this remains a speculative hypothesis (as does the alternative treatment of Ref. 19, which is entirely based on the idea that $\Delta G = \lambda$). Transient spectroscopic studies in an applied

electric field, described in the previous section, may be able to address this issue by providing a variation of ΔG.

The simulations of Warshel and co-workers are of relevance to the question of the magnitude of the protein reorganization energy in the RC. For the primary reaction, these workers found that the reorganization energy was very small. This result is compatible with the above discussion. An interesting question is whether similar values would be found for other ET reactions in the RC, at least with regard to the low frequency modes. As more simulations are reported, we can expect to obtain more detailed and reliable answers to these sort of questions.

V-D. A proposed physical picture of charge separation

We summarize here our proposed physical picture of the primary charge separation process, based on the analyses described above. The initially prepared P* state is assumed to be a quasiresonant superposition of a Q_y exciton state and a close-lying internal charge transfer state of the SP, the combined manifolds of which make up the P* band. Via the CT configuration, the excited state has a reasonably strong coupling (50–100 cm^{-1}) to the intermediate virtual state P^+B^-, which in turn is coupled to P^+H^-. This superexchange pathway leads to an effective coupling of P* with P^+H^- of about 20 cm^{-1}, leading to the experimentally observed picosecond charge separation. On the other hand, the back-reaction of P^+H^- to the ground state of P is not effectively connected to this pathway. The small reorganization energy of the primary step also may place the back reaction in the inverted region (in the sense of Marcus theory); this, combined with the above-mentioned electronic factor, explains the orders of magnitude reduction in rate of recombination as compared to charge separation.

The strength of this model is that it simultaneously explains (at least qualitatively) the Stark effect, hole-burning measurements, and singlet-triplet splitting data, as well as the failure to observe a new CT state at high energy. It is also consistent with the heterodimer results; if the interpretations of these experiments can be verified unambiguously, they provide direct evidence of the participation of the internal CT state in the primary process, as well as an estimate of the position of this state in native RCs (by extrapolating from the modified system to the natural one). On the other hand, there are some difficulties faced by the model (e.g., the apparent single-band nature of the Stark spectrum) and future experimental tests (resonance Raman) which have to be addressed.

If correct, this picture should be of considerable values to chemists attempting to design synthetic analogs of the RC. If one could tune a charge transfer state into near reasonance with an excited state, and then have this charge transfer state couple into a long range superexchange pathway to the acceptor, one might be able to enhance the forward reaction without promoting rapid recombination.

This proposal is by no means the first suggestion that charge separation in the SP is substantial and is relevant to the functioning of the RC; ideas along these lines were in fact described by Thurnauer et al. in 1975 [135]. What we have tried to provide is (1) a hypothesis as to the function the CT state serves in ensuring the efficiency of charge separation, and (2) a detailed examination of the consequences of assumptions concerning the energetics and coupling of the state for various experimental measurements.

VI. Conclusion

It is clear that the photosynthetic reaction center will be fertile ground for biophysical research for many years to come. Even if the basic features of the underlying mechanism of primary charge separation are determined, construction of a complete, detailed theoretical description of the system will be a lengthy and demanding task. As the first membrane-bound, electron transport protein to be crystallized, the RC will then serve as a theoretical laboratory in which to test the accuracy of molecular level models of such proteins.

At present, the initial task of understanding primary charge separation, even on a crude phenomenological level, is far from complete. A minimal description which could be said to fulfill this role would specify the following information: (1) energy level scheme and approximate coupling strengths for all participant chromophore electronic configurations; (2) sequence of electron transfer events; degree of adiabaticity of each step in the charge separation process; (3) microscopic cause of inactivation of the M branch of the RC, (4) numerical values of the chromophore and protein reorganization energy, and a physical picture of each. None of these issues have been definitely resolved as of yet.

On the other hand, we now have a number of concrete proposals which can be subjected to further experimental tests. Site-directed mutagenesis [11–14], in particular, when coupled with the array of physical techniques described above, should provide a constant supply of new experimental results with which to confront theory. Indeed, as genetic manipulations become more straightforward it is quite likely that the bottleneck in obtaining useful results will shift from the generation of interesting mutants to performance and interpretation of physical experiments.

Acknowledgements

Support from the NIH and the NSF is acknowledged. R.A.F. is a Camille and Henry Dreyfus

Teacher-Scholar and the recipient of a Research Career Development Award from the NIH, Institute of General Medical Sciences. We thank many of our colleagues in photosynthesis for useful discussions and preprints of relevant papers.

References

1 Deisenhofer, J., Epp, O., Miki, K., Huber, R. and Michel, H. (1984) J. Mol. Biol. 180, 385–398.
2 Michel, H., Epp, O. and Deisenhofer, J. (1986) EMBO J. 5, 2445–2451.
3 Deisenhofer, J., Epp, O., Miki, K., Huber, R. and Michel, H. (1985) Nature 318, 618–624.
4 Chang, C.H., Tiede, D.M., Tang, J., Smith, U., Norris, J.R. and Schiffer, M. (1986) FEBS Lett. 205, 82–86.
5 Allen, J.P., Feher, G., Yeates, T.O., Komiya, H. and Rees, D.C. (1987) Proc. Natl. Acad. Sci. USA 84, 5730–5734.
6 Allen, J.P., Feher, G., Yeates, T.O., Komiya, H. and Rees, D.C. (1987) Proc. Natl. Acad. Sci. USA 84, 6162–6166.
7 Allen, J.P., Feher, G., Yeates, T.O., Komiya, H. and Rees, D.C. (1987) Proc. Natl. Acad. Sci. USA 84, 6438–6442.
8 Allen, J.P., Feher, G., Yeates, T.O., Komiya, H. and Rees, D.C. (1988) Proc. Natl. Acad. Sci. USA 85, 8487–8491.
9 Wasielewski, M.R. (1988) Photochem. Photobiol. 47, 923–929.
10 Maroti, P., Kirmaier, C., Wraight, C., Holten, D. and Pearlstein, R.M. (1985) Biochim. Biophys. Acta 810, 132–139.
11 Bylina, E.J. and Youvan, D.C. (1987) Z. Naturforsch. C 42, 769–774.
12 Bylina, E.J. and Youvan, D.C. (1988) Proc. Natl. Acad. Sci. USA 85, 7226–7230.
13 Bylina, E.J., Jovine, R. and Youvan, D.C. (1988) in Photosynthetic Bacterial Reaction Center: Structure and Dynamics, NATO ASI Series, Series A: Life Sciences Vol. 149 (Breton, J. and Vermèglio, A., eds.), pp. 113–118, Plenum, New York.
14 Kirmaier, C., Holten, D., Bylina, E.J. and Youvan, D.C. (1988) Proc. Natl. Acad. Sci. USA 85, 7562–7566.
15 Kirmaier, C. and Holten, D. (1987) Photosynth. Res. 13, 225–260.
16 Parson, W.W. (1982) Annu. Rev. Biophys. Bioeng. 11, 57–80.
17 Shuvalov, V.A., Asadov, A.A. (1979) Biochim. Biophys. Acta 545, 296–308.
18 Phillipson, K.D., Sauer, K. (1973) Biochemistry 12, 535–539.
19 Martin, J.L., Breton, J., Lambry, J.C. and Fleming, G. (1988) in Photosynthetic Bacterial Reaction Center: Structure and Dynamics, Vol. 149 (Breton, J. and Vermèglio, A., eds.), pp. 195–203, Plenum, New York.
20 Fleming, G.R., Martin, J.L. and Breton, J. (1988) Nature 333, 190–192.
21 Woodbury, N.W., Parson, W.W., Gunner, M.R., Prince, R.C. and Dutton, P.L. (1986) Biochim. Biophys. Acta 851, 6–22.
22 Martin, J.L., Breton, J., Hoff, A.J., Migus, A. and Antonetti, A. (1986) Proc. Natl. Acad. Sci. USA 83, 957–961.
23 Breton, J., Martin, J.L., Migus, A., Antonetti, A. and Orszag, A. (1986) Proc. Natl. Acad. Sci. USA 83, 5121–5125.
24 Breton, J., Martin, J.L., Petrich, J., Migus, A. and Antonetti, A. (1986) FEBS Lett. 209, 37–43.
25 Holten, D., Windsor, M.W., Parson, W.W. and Thornberg, J.P. (1978) Biochim. Biophys. Acta 501, 112–126.
26 Goutermann, M. (1978) in The Porphyrins, Vol. 3 (Dolphin, D., ed.), pp. 1–165, Academic Press, New York.
27 Warshel, A. (1979) J. Am. Chem. Soc. 101, 744–746.
28 Knapp, E.W., Fischer, S.F., Zinth, W., Sander, M., Kaiser, W., Deisenhofer, J. and Michel, H. (1985) Proc. Natl. Acad. Sci. USA 82, 8463–8467.
29 Hanson, L.K., Fajer, J. and Thompson, M. (1987) in Progress in Photosynthesis Research, Vol. I (Biggins, J., ed.), pp. 311–331, Martinus Nijhoff, Dordrecht.
30 Kashiwaga, H., Hirota, F., Nagashima, U. and Takada, T. (1986) Int. J. Quantum Chem. 30, 311–326.
31 Friesner, R.A. (1985) Chem. Phys. Lett. 116, 39–43.
32 Friesner, R.A. (1986) J. Chem. Phys. 85, 1462–1468.
33 Friesner, R.A. (1986) J. Chem. Phys. 86, 3522–3531.
34 Friesner, R.A. (1986) J. Phys. Chem. 92, 3091–3096.
35 Bardeen, J., Cooper, L.N. and Schrieffer, J.R. (1957) Phys. Rev. 108, 1175–1204.
36 Halley, J.W. ed. (1988) Theories of High Temperature Superconductivity, Addison-Wesley, New York.
37 Warshel, A. and Parson, W.W. (1987) J. Am. Chem. Soc. 109, 6143–6152.
38 Parson, W.W. and Warshel, A. (1987) J. Am. Chem. Soc. 109, 6152–6163.
39 Parson, W.W., Warshel, A. and Creighton, S. (1988) J. Phys. Chem. 92, 2696–2701.
40 Hanson, L.K., Fajer, J., Thompson, M.A. and Zerner, M. (1987) J. Am. Chem. Soc. 109, 4728.
41 Barkigia, K., Chantranupong, L., Kehres, L.A., Smith, K.M. and Fajer, J. (1988) in Photochemical Solar Energy (Norris, J.R., ed.), Elsevier, New York.
42 Plato, M., Tränkle, E., Lubitz, W., Lendzian, F. and Möbius, K. (1986) Chem. Phys. 107, 185–196.
43 Fischer, S.F. and Scherer, P.O.J. (1987) Chem. Phys. 115, 151–158.
44 Eccles, J., Honig, B. and Schulten, K. (1988) Biophys. J. 53, 137–144.
45 Hanson, L.K. (1988) Photochem. Photobiol. 47, 903–921.
46 Plato, M. and Winscom, C.J. (1988) in Photosynthetic Bacterial Reaction Center: Structure and Dynamics, NATO ASI Series, Series A: Life Sciences Vol. 149 (Breton, J. and Vermèglio, A., eds.), pp. 421–424, Plenum, New York.
47 Creighton, S., Hwang, J.K., Warshel, A., Parson, W.W. and Norris, J. (1988) Biochemistry 27, 774–781.
48 Bixon, M. and Lifson, S. (1966) Biopolymers 4, 815–821.
49 Lifson, S. and Warshel, A. (1968) J. Chem. Phys. 49, 5116–5129.
50 Levitt, M. and Lifson, S. (1969) J. Mol. Biol. 46, 269–279.
51 McCammon, J.A., Gelin, B.R. and Karplus, M. (1977) Nature 267, 585–590.
52 Lybrand, T.P., McCammon, J.A. and Wipf, G. (1986) Proc. Natl. Acad. Sci. USA 83, 833–835.
53 Northrup, S.H., Pear, M.R., Morgan, J.D., McCammon, J.A. and Karplus, M. (1981) J. Mol. Biol. 153, 1087–1109.
54 Levy, R.M. and Karplus, M. (1983) Adv. Chem. Ser. 204, 445–468.
55 Parson, W.W., Warshel, A., Creighton, S. and Norris, J. (1988) in Photosynthetic Bacterial Reaction Center: Structure and Dynamics, NATO ASI Series, Series A: Life Sciences Vol. 149 (Breton, J. and Vermèglio, A., eds.), pp. 309–317, Plenum, New York.
56 Treutlein, H., Schulten, K., Deisenhofer, J., Michel, H., Brünger, A. and Karplus, M. (1988) in Photosynthetic Bacterial Reaction Center: Structure and Dynamics, Vol. 149 (Breton, J. and Vermèglio, A., eds.), pp. 139–150, Plenum, New York.
57 Treutlein, H., Schulten, K., Niedermeier, C., Deisenhofer, J., Michel, H. and DeVault, D. (1988) in PHotosynthetic Bacterial Reaction Center: Structure and Dynamics, Vol. 149 (Breton, J. and Vermèglio, A., eds.), pp. 369–377, Plenum, New York.
58 Knapp, E.W., Scherer, P.O.J. and Fischer, S.F. (1986) Biochim. Biophys. Acta 852, 295–305.
59 Knapp, E.W., Fischer, S.F. (1985) in Antennas and Reaction Centers of Photosynthetic Bacteria – Structures, Interactions and Dynamics, Springer Series in Chemical Physics, vol. 42 (Michel-Beyerle, M.E., ed.), pp. 103–108, Springer, Berlin.
60 Marcus, R.A. and Sutin, N. (1985) Biochim. Biophys. Acta 811, 265–322.
61 Marcus, R.A. (1987) Chem. Phys. Lett 133, 471–477.

62 Marcus, R.A. (1988) Chem. Phys. Lett 146, 13–22.
63 Marcus, R.A. (1988) in Photosynthetic Bacterial Reaction Center: Structure and Dynamics, Vol. 149 (Breton, J. and Vermèglio, A., eds.), pp. 389–398, Plenum, New York.
64 Michel-Beyerle, M.E., Plato, M., Deisenhofer, J., Michel, H., Bixon, M. and Jortner, J. (1988) Biochim. Biophys. Acta 932, 52–70.
65 Ogrodnik, A., Remy-Richter, N., Michel-Beyerle, M.E. and Feick, R. (1987) Chem. Phys. Lett. 135, 576–581.
66 Bixon, M., Jortner, J., Michel-Beyerle, M.E., Orgodnik, A. and Lersch, W. (1987) Chem. Phys. Lett. 140, 626–630.
67 Won, Y. and Friesner, R.A. (1988) Biochim. Biophys. Acta 935, 9–18.
68 Won, Y. and Friesner, R.A. (1988) J. Phys. Chem. 92, 2208–2214.
69 Won, Y. and Friesner, R.A. (1988) J. Phys. Chem. 92, 2214–2219.
70 Won, Y. and Friesner, R.A. (1987) Proc. Natl. Acad. Sci. USA 84, 5511–5515.
71 Won, Y. and Friesner, R.A. (1988) in Photosynthetic Bacterial Reaction Center: Structure and Dynamics, Vol. 149 (Breton, J. and Vermèglio, A., eds.), pp. 341–349, Plenum, New York.
72 Scherer, P.O.J., Fischer, S.F., Hörber, J.K.H., Michel-Beyerle, M.E., Michel, H. (1985) in Antennas and Reaction Centers of Photosynthetic Bacteria – Structures, Interactions and Dynamics, Springer Series in Chemical Physics, Vol. 42 (Michel-Beyerle, M.E., ed.), pp. 131–137, Springer, Berlin.
73 Hayes, J.M. and Small, G.J. (1986) J. Phys. Chem. 90, 4928–4931.
74 Hayes, J.M., Gillie, J.K., Tang, D. and Small, G.J. (1988) Biochim. Biophys. Acta 932, 287–305.
75 Even, U., Magen, J. and Jortner, J. (1982) Chem. Phys. Lett. 88, 131–134.
76 Platenkamp, R.J., Den Blanken, H.J. and Hoff, A.J. (1980) Chem. Phys. Lett. 76, 35–41.
77 Warshel, A. (1980) Proc. Natl. Acad. Sci. USA 77, 3105–3109.
78 Norris, J.R., Bowman, M.K., Budil, D.E., Tang, J., Wraight, C.A. and Closs, G.L. (1982) Proc. Natl. Acad. Sci. USA 79, 5532–5536.
79 Norris, J.R., Lin, C.P. and Budil, D.E. (1987) J. Chem. Soc., Faraday Trans. 1, 83, 13–27.
80 Moehl, K.W., Lous, E.J. and Hoff, A.J. (1985) Chem. Phys. Lett. 121, 22–27.
81 Chidsey, C.E.D., Takiff, L., Goldstein, R.A. and Boxer, S.G. (1985) Proc. Natl. Acad. Sci. USA 82, 6850–6854.
82 Goldstein, R.A., Takiff, L. and Boxer, S.G. (1988) Biochim. Biophys. Acta 934, 253–263.
83 Vermeglio, A. and Paillotin, G. (1982) Biochim. Biophys. Acta 681, 32–40.
84 Breton, J. (1985) in Antennas and Reaction Centers of Photosynthetic Bacteria – Structures Interactions and Dynamics, Springer Series in Chemical Physics, vol. 42 (Michel-Beyerle, M.E., ed.), pp. 109–121, Springer, Berlin.
85 Breton, J. (1986) Biochim. Biophys. Acta 810, 235–245.
86 Breton, J. (1988) in Photosynthetic Bacterial Reaction Center: Structure and Dynamics, Vol. 149 (Breton, J. and Vermèglio, A., eds.), pp. 59–69, Plenum, New York.
87 Lockhart, D.J. and Boxer, S.J. (1987) Biochemistry 26, 664–668.
88 Lockhart, D.J. and Boxer, S.J. (1988) Chem. Phys. Lett. 144, 243–250.
89 Parson, W.W., Scherz, A. and Warshel, A. (1985) in Antennas and Reaction Centers of Photosynthetic Bacteria – Structures, Interactions and Dynamics, Springer Series in Chemical Physics, Vol. 42 (Michel-Beyerle, M.E., ed.), pp. 122–130, Springer, Berlin.
90 Zinth, W., Sander, M., Dobler, J., Kaiser, W., Michel, H. (1985) in Antennas and Reaction Centers of Photosynthetic Bacteria – Structures, Interactions and Dynamics, Springer Series in Chemical Physics, Vol. 42 (Michel-Beyerle, M.E., ed.), pp. 97–102, Springer, Berlin.
91 Kirmaier, C. and Holten, D. (1988) in Photosynthetic Bacterial Reaction Center: Structure and Dynamics, Vol. 149 (Breton, J. and Vermèglio, A., eds.), pp. 219–228, Plenum, New York.
92 Hoff, A.J. (1988) in Photosynthetic Bacterial Reaction Center: Structure and Dynamics, NATO ASI Series, Series A: Life Sciences, Vol. 149 (Breton, J. and Vermèglio, A., eds.), pp. 89–97, Plenum, New York.
93 Won, Y. and Friesner, R.A. (1989) Isr. J. Chem., in press.
94 DeLeeuw, D., Malley, M., Butterman, G., Okamura, M.Y. and Fisher, G. (1982) Biophys. J. 37, 111a.
95 Lösche, M., Feher, G. and Okamura, M.Y. (1987) Proc. Natl. Acad. Sci. USA 84, 7537–7541.
96 Boxer, S.G., Lockhard, D.J. and Middendorf, T.R. (1986) Chem. Phys. Lett. 123, 476–482.
97 Boxer, S.G., Midendorf, T.R. and Lockhart, D.J. (1986) FEBS Lett. 200, 237–241.
98 Meech, S.R., Hoff, A.J. and Wiersma, D.A. (1985) Chem. Phys. Lett. 121, 287–292.
99 Völker, S. and Macfarlane, R.M. (1980) J. Chem. Phys. 73, 4476–4482.
100 Boxer, S.J., Gottfried, D.S., Lockhart, D.J. and Middendorf, T.R. (1987) J. Chem. Phys. 86, 2439–2441.
101 Smalley, R.F. (1983) Annu. Rev. Phys. Chem. 34, 129–153.
102 Friesner, R. and Silbey, R. (1981) J. Chem. Phys. 74, 1166–1172.
103 Tang, D., Jankowiak, R., Gillie, J.K., Small, G.J. and Tiede, D.M. (1988) J. Phys. Chem. 92, 4012–4015.
104 Scherz, A. and Parson, W.W. (1984) Biochim. Biophys. Acta 766, 666–678.
105 Scherer, P.O.J. and Fischer, S.F. (1987) Chem. Phys. Lett. 141, 179–185.
106 Scherer, P.O.J. and Fischer, S.F. (1988) in Photosynthetic Bacterial Reaction Center: Structure and Dynamics, NATO ASI Series, Series A: Life Sciences, Vol. 149 (Breton, J. and Vermèglio, A., eds.), pp. 425–433, Plenum, New York.
107 Shuvalov, V.A. and Parson, W.W. (1981) Proc. Natl. Acad. Sci. USA 78, 957–961.
108 Bixon, M., Jortner, J., Plato, M. and Michel-Beyerle, M.E. (1988) in Photosynthetic Bacterial Reaction Center: Structure and Dynamics, NATO ASI Series, Series A: Life Sciences, Vol. 149 (Breton, J. and Vermèglio, A., eds.), pp. 399–419, Plenum, New York.
109 Warshel, A. and Hwang, J.-K. (1986) J. Chem. Phys. 84, 4938–4957.
110 Feher, G., Arno, T.R. and Okamura, M.Y. (1988) in Photosynthetic Bacterial Reaction Center: Structure and Dynamics, Vol. 149 (Breton, J. and Vermèglio, A., eds.), pp. 271–287, Plenum, New York.
111 Popovic, Z.D., Kovacs, G.J., Vincett, P.S. and Dutton, P.L. (1985) Chem. Phys. Lett 116, 405–410.
112 Popovic, Z.D., Kovacs, G.J., Vincett, P.S., Alegria, G. and Dutton, P.L. (1986) Biochim. Biophys. Acta 851, 38–48.
113 Dutton, P.L., Alegria, G. and Gunner, M.R. (1988) in Photosynthetic Bacterial Reaction Center: Structure and Dynamics, Vol. 149 (Breton, J. and Vermèglio, A., eds.), pp. 185–194, Plenum, New York.
114 Bixon, M. and Jortner, J. (1988) J. Phys. Chem. 92, 7148–7156.
115 Gunner, M.R., Robertson, D.E. and Dutton, P.L. (1986) J. Phys. Chem. 90, 3783–3795.
116 Gunner, M.R. and Dutton, P.L. (1988) in Photosynthetic Bacterial Reaction Center: Structure and Dynamics, NATO ASI Series, Series A: Life Sciences, Vol. 149 (Breton, J. and Vermèglio, A., eds.), pp. 259–269, Plenum, New York.
117 Davis, M.S., Forman, A., Hanson, L.K., Thornber, J.P. and Fajer, J. (1979) J. Phys. Chem. 83, 3325–3332.
118 Bylina, E.J., Kirmaier, C., McDowell, L. Holten, D. and Youvan, D.C. (1988) Nature 336, 182–184.
119 Wasliewski, M. and Tiede, D. (1986) FEBS Lett. 204, 368–372.
120 Kirmaier, C. and Holten, D. (1988) FEBS Lett. 239, 211–218.
121 Woodbury, N., Becker, M., Middendorf, D., Parson, W.W. (1985) Biochemistry 24, 7516–7521.

122 DiMagno, T.J., Bylina, E.J., Angerhofer, A., Youvan, D.C. and Norris, J.R. (1989) Biochemistry, submitted
123 Reference deleted.
124 Takiff, L. and Boxer, S.G. (1988) Biochim. Biophys. Acta 932, 325–334.
125 Lockhart, D., Goldstein, R. and Boxer, S.G. (1988) J. Chem. Phys. 89, 1405–1415.
126 Warshel, A., Sussman, F. and King, G. (1986) Biochemistry 25, 8368–8372.
127 Churg, A.K. and Warshel, A. (1986) Biochemistry 25, 1675–1680.
128 Russell, S.T. and Warshel, A. (1985) J. Mol. Biol. 185, 389–404.
129 Budil, D., Gast, P., Chang, C.H., Schiffer, M. and Norris, J.R. (1987) Ann. Rev. Phys. Chem. 38, 561–583.
130 Komyia, H., Yeates, T.O., Rees, D.C., Allen, J.P. and Feher, G. (1988) Proc. Natl. Acad. Sci. USA 85, 9012–9016.
131 Goldstein, R.A., Takiff, L. and Boxer, S.G. (1988) Biochim. Biophys. Acta 934, 253–263.
132 Won, Y. and Friesner, R.A. (1988) in Photosynthetic Bacterial Reaction Center: Structure and Dynamics, NATO ASI Series, Series A: Life Sciences Vol. 149 (Breton, J. and Vermèglio, A., eds.), pp. 341–351, Plenum, New York.
133 Lockhart, D. and Boxer, (1988) Proc. Natl. Acad. Sci. USA 85, 107–111.
134 Kirmaier, C., Bylina, E., Youvan, D.C. and Holten, D. (1989) Chem. Phys. Lett., in press.
135 Thurnauer, M., Katz, J.J. and Norris, J.R. (1975) Proc. Natl. Acad. Sci. USA 72, 3270–3274.